

Partition Trees: Conditional Density Estimation over General Outcome Spaces

Felipe Angelim¹ Alessandro Leite²

Abstract

We propose *Partition Trees*, a tree-based framework for conditional density estimation over general outcome spaces, supporting both continuous and categorical variables within a unified formulation. Our approach models conditional distributions as piecewise-constant densities on data-adaptive partitions and learns trees by directly minimizing conditional negative log-likelihood. This yields a scalable, nonparametric alternative to existing probabilistic trees that does not make parametric assumptions about the target distribution. We further introduce *Partition Forests*, an ensemble extension obtained by averaging conditional densities. Empirically, we demonstrate improved probabilistic prediction over CART-style trees and competitive or superior performance compared to state-of-the-art probabilistic tree methods and Random Forests, along with robustness to redundant features and heteroscedastic noise.

1. Introduction

Decision trees are among the earliest and most widely used learning algorithms, valued for their computational efficiency, interpretability, and ability to capture nonlinear interactions through recursive partitioning (Morgan & Sonquist, 1963; Kass, 1980; Breiman et al., 2017; Loh, 2014). Early methods such as Automatic Interaction Detection (AID) (Morgan & Sonquist, 1963) and CHAID (Kass, 1980) introduced the idea of fitting piecewise-constant models on data-adaptive partitions of the input space. The CART framework later systematized tree construction for both classification and regression and popularized pruning via cost-complexity regularization (Breiman et al., 2017).

Although classical trees focus on point prediction or class probabilities, there has been growing interest in extend-

ing tree-based methods to probabilistic prediction and conditional density estimation. Recent approaches include CADET (Cousins & Riondato, 2019), which employs parametric conditional densities at the leaves and selects splits using a cross-entropy criterion, and CDTree (Yang & van Leeuwen, 2024), which jointly optimizes splits and leaf-wise histograms via a minimal description length objective. Although these methods demonstrate strong empirical performance, CADET’s leaf models impose parametric assumptions, whereas CDTree’s joint split-and-histogram optimization can be computationally demanding, limiting scalability on large datasets.

In this paper, we introduce *Partition Trees*, a tree-based framework for conditional density estimation over general outcome spaces that supports both continuous and categorical variables. Our approach models conditional distributions as piecewise-constant densities defined on data-adaptive partitions of the joint covariate-outcome space. Formally, we adopt a measure-theoretic perspective in which conditional densities are defined via probability measures and Radon–Nikodym derivatives with respect to these partitions. Within this unified framework, both classification and regression emerge as cases of conditional density estimation. Trees are constructed greedily by maximizing an empirical log-loss objective, which is equivalent to minimizing the conditional negative log-likelihood of the resulting density estimator. This objective naturally accommodates heteroscedastic noise and leads to empirical robustness to redundant features.

We further extend *Partition Trees* to ensembles, termed *Partition Forests*, by averaging the predicted conditional densities across multiple trees. Experiments on a diverse set of classification and regression benchmarks demonstrate that *Partition Forests* consistently improve probabilistic prediction compared to CART-style trees. On classification tasks, they achieve lower log-loss on several datasets, while *Partition Forests* outperform Random Forests on the majority of benchmarks. For regression, *Partition Forests* provide competitive point predictions and provide strong probabilistic performance, outperforming CADET on larger datasets without relying on parametric assumptions. Finally, semi-synthetic experiments highlight robustness to both homoscedastic and heteroscedastic noise, and to redundant features. We provide an im-

¹Independent Researcher, felipeangelim.com ²INSA Rouen Normandy, Normandy University, LITIS, Rouen, France. Correspondence to: Felipe Angelim <felipeangelim@gmail.com>, Alessandro Leite <aleite@insa-rouen.fr>.

plementation of *Partition Trees* and *Partition Forests* at github.com/felipeangelimvieira/partition_tree.

2. Methodology

2.1. Setting

Let $(\Omega, \mathcal{A}, \mathbb{P})$ be a probability space. Let $X \in \mathcal{X}$ denote the covariates and $Y \in \mathcal{Y}$ is the outcome. We observe a dataset $\mathcal{D} = \{(x_i, y_i)\}_{i=1}^N$ of i.i.d. samples drawn from the joint distribution \mathbb{P}_{XY} , the push-forward of \mathbb{P} on the product space $\mathcal{Z} := \mathcal{X} \times \mathcal{Y}$.

A measurable cell $A \subseteq \mathcal{Z}$ is written as a product set $A = A_X \times A_Y$, where $A_X \subseteq \mathcal{X}$ and $A_Y \subseteq \mathcal{Y}$ denote its covariate and outcome components, respectively. We use subscripts to indicate projections of a cell onto a specific coordinate space, and omit subscripts when referring to subsets of the joint space. Let $\text{pr}_X : \mathcal{X} \times \mathcal{Y} \rightarrow \mathcal{X}$ and $\text{pr}_Y : \mathcal{X} \times \mathcal{Y} \rightarrow \mathcal{Y}$ denote the canonical coordinate projections. Accordingly, for any $A \subseteq \mathcal{X} \times \mathcal{Y}$, we define $A_X := \text{pr}_X(A)$ and $A_Y := \text{pr}_Y(A)$. Let

$$n_{XY}(A) := \sum_{i=1}^N \mathbf{1}\{(x_i, y_i) \in A\} = N \hat{\mathbb{P}}_{XY}(A) \quad (1)$$

$$n_X(A) := \sum_{i=1}^N \mathbf{1}\{x_i \in A_X\} = N \hat{\mathbb{P}}_X(A_X) \quad (2)$$

denote the number of samples on a cell and its \mathcal{X} and \mathcal{Y} components. We use $\mathbb{P}_X(A) := \mathbb{P}_X(A_X)$, $\mathbb{P}_Y(A) := \mathbb{P}_Y(A_Y)$, $\mu_Y(A) := \mu_Y(A_Y)$ for simplicity. In addition, let $\pi_N(\{z_i\}_{i=1}^N)$, $z_i \in \mathcal{Z}$, be a partitioning rule that maps datasets of size N to measurable partitions $\pi_N(\{z_i\}_{i=1}^N) = \{A_i\}_{i=1}^K$. We overload the usage of π_N to also represent a partition generated by $\pi_N(\{z_i\}_{i=1}^N)$ when the dataset is fixed or irrelevant to the context. In particular, $\pi_N(\mathcal{D})$ implies that $|\mathcal{D}| = N$. For any $z \in \mathcal{Z}$, we denote by $\pi_N[z]$ the unique cell $A \in \pi_N$ such that $z \in A$.

2.2. Mixed-Type Covariates and Outcomes

We allow \mathcal{X} and \mathcal{Y} to contain a mixture of coordinate types.

$$X = (X^{(c)}, X^{(k)}) \in \mathcal{X}^{(c)} \times \mathcal{X}^{(k)} =: \mathcal{X}$$

$$Y = (Y^{(c)}, Y^{(k)}) \in \mathcal{Y}^{(c)} \times \mathcal{Y}^{(k)} =: \mathcal{Y}$$

where,

(a) $\mathcal{X}^{(c)} \subseteq \mathbb{R}^{d_{x,c}}$ and $\mathcal{Y}^{(c)} \subseteq \mathbb{R}^{d_{y,c}}$ are continuous coordinates;

(b) $\mathcal{X}^{(k)} = \prod_{j=1}^{d_{x,k}} \Sigma_{x,j}$ and $\mathcal{Y}^{(k)} = \prod_{j=1}^{d_{y,k}} \Sigma_{y,j}$ are categorical coordinates with alphabets $\Sigma_{x,j}, \Sigma_{y,j}$ (assumed finite).

Cells are factorized coordinate-wise, with internal splits for continuous coordinates, and subset splits for categorical

coordinates.

We introduce some notions that will be important in the consistency theorem. We first define a distance metric for continuous coordinates. To handle unbounded continuous domains, we use the transformation $\phi(u) = u/(1+u)$ on the Euclidean distance.

Define $d_{\text{cont}}(z, z') = \phi(\|(x^{(c)}, y^{(c)}) - (x'^{(c)}, y'^{(c)})\|_2)$ and $\text{diam}_{\text{cont}}(A) = \sup_{z, z' \in A} d_{\text{cont}}(z, z')$. Also, define the diameter:

$$\text{diam}(A) = \text{diam}_{\text{cont}}(A) + \sum_k \frac{|S_k(A)| - 1}{|\Sigma_k| - 1}.$$

where $S_k(A) \subseteq \Sigma_k$ is the set of categories present in leaf A along categorical coordinate k .

2.3. Conditional Density Estimation via Radon–Nikodym Derivatives

Let (X, Y) be a random pair taking values in $\mathcal{X} \times \mathcal{Y}$, where \mathcal{X} and \mathcal{Y} are measurable spaces. Let \mathbb{P}_{XY} and \mathbb{P}_X denote the joint and marginal distributions, respectively. We fix a σ -finite reference measure μ_Y on \mathcal{Y} , chosen as the counting measure for discrete outcomes and Lebesgue measure for continuous ones.

Existence of a conditional density. We assume throughout that the joint distribution admits a conditional density of Y given X with respect to μ_Y .

Assumption 2.1 (Existence of conditional density). The joint distribution \mathbb{P}_{XY} is absolutely continuous with respect to $\mathbb{P}_X \otimes \mu_Y$, i.e.,

$$\mathbb{P}_{XY} \ll \mathbb{P}_X \otimes \mu_Y$$

Under Assumption 2.1, the Radon–Nikodym derivative

$$f := \frac{d\mathbb{P}_{XY}}{d(\mathbb{P}_X \otimes \mu_Y)}$$

exists and defines a version of the conditional density of Y given X with respect to μ_Y , in the sense that for \mathbb{P}_X -almost every x and all measurable $B \subseteq \mathcal{Y}$,

$$\mathbb{P}(Y \in B \mid X = x) = \int_B f(x, y) \mu_Y(dy).$$

2.3.1. PIECEWISE-CONSTANT APPROXIMATION ON A PARTITION

Define $\nu := \mathbb{P}_X \otimes \mu_Y$ and let $\bar{\mathcal{Z}} \subseteq \mathcal{Z}$ be a measurable subset with $\nu(\bar{\mathcal{Z}}) < \infty$. When $\nu(\mathcal{Z}) < \infty$, one may take $\bar{\mathcal{Z}} = \mathcal{Z}$. Let π be a measurable partition of $\bar{\mathcal{Z}}$ into cells $A = A_X \times A_Y$.

On a cell A with $0 < \nu(A) < \infty$, the best constant approximation of f in the sense of matching the \mathbb{P}_{XY} -mass of the cell is obtained by choosing $c_A \geq 0$ such that

$$\int_A c_A \nu(dz) = \mathbb{P}_{XY}(A).$$

Solving gives the cell-average value

$$c_A = \frac{\mathbb{P}_{XY}(A)}{\nu(A)}. \quad (3)$$

This yields the piecewise-constant estimator

$$f_\pi(z) = \begin{cases} \frac{\mathbb{P}_{XY}(\pi[z])}{\nu(\pi[z])}, & z \in \bar{\mathcal{Z}}, \\ 0, & \text{otherwise.} \end{cases} \quad (4)$$

Equivalently, $f_\pi = \mathbb{E}_\nu[f \mid \sigma(\pi)]$ ν -a.e. on $\bar{\mathcal{Z}}$, i.e., the conditional expectation of f given the σ -algebra generated by the partition.

Because $\nu = \mathbb{P}_X \otimes \mu_Y$ factorizes over X and Y , a product cell $A = A_X \times A_Y$ satisfies

$$\nu(A) = \mathbb{P}_X(A_X) \mu_Y(A_Y),$$

so (3) can be written more explicitly as

$$c_A = \frac{\mathbb{P}_{XY}(A)}{\mathbb{P}_X(A_X) \mu_Y(A_Y)}.$$

2.3.2. EMPIRICAL ESTIMATOR FROM COUNTS

We estimate $\mathbb{P}_{XY}(A)$ and $\mathbb{P}_X(A_X)$ from the sample $\mathcal{D} = \{(x_i, y_i)\}_{i=1}^N$. Recall the counts defined in Equations (1) and (2). Then $\hat{\mathbb{P}}_{XY}(A) = n_{XY}(A)/N$ and $\hat{\mathbb{P}}_X(A_X) = n_X(A)/N$, and the plug-in estimate of c_A becomes

$$\hat{c}_A = \frac{\hat{\mathbb{P}}_{XY}(A)}{\hat{\mathbb{P}}_X(A_X) \mu_Y(A_Y)} = \frac{n_{XY}(A)}{n_X(A) \mu_Y(A_Y)}, \quad (5)$$

defined whenever $n_X(A) > 0$ and $\mu_Y(A_Y) > 0$. Substituting (5) into (4) yields a fully explicit estimator once a partition π_N is fixed.

2.3.3. TRUNCATION OF UNBOUNDED OUTCOME SPACES

If $\mu_Y(\mathcal{Y}) = \infty$ (e.g., \mathcal{Y} contains an unbounded continuous component), then $\nu(A) = \mathbb{P}_X(A_X) \mu_Y(A_Y)$ may be infinite unless A_Y has finite μ_Y -measure. To ensure well-defined denominators while still covering most of the probability mass, we restrict the estimator to a data-dependent truncated outcome domain $\bar{\mathcal{Y}}_N$ with $\mu_Y(\bar{\mathcal{Y}}_N) < \infty$, and define $\bar{\mathcal{Z}}_N := \mathcal{X} \times \bar{\mathcal{Y}}_N$.

For N samples $\{y_i^{(c)}\}_{i=1}^N$ in the continuous part $\mathcal{Y}^{(c)} \subseteq \mathbb{R}^{d_{y,c}}$, define the axis-aligned box

$$\bar{\mathcal{Y}}_N^{(c)} := \prod_{j=1}^{d_{y,c}} [\underline{y}_{N,j} - \delta_N, \bar{y}_{N,j} + \delta_N], \quad (6)$$

$$\underline{y}_{N,j} := \min_{1 \leq i \leq N} y_{i,j}, \quad \bar{y}_{N,j} := \max_{1 \leq i \leq N} y_{i,j},$$

and set $\bar{\mathcal{Y}}_N := \bar{\mathcal{Y}}_N^{(c)} \times \mathcal{Y}^{(k)}$ for the mixed case. The padding $\delta_N > 0$ (typically $\delta_N \downarrow 0$) avoids boundary effects and ensures $\mu_Y(\bar{\mathcal{Y}}_N) < \infty$.

Given a data-dependent partition π_N of $\bar{\mathcal{Z}}_N$, our estimator is

$$\hat{f}_{\pi_N}(z) = \begin{cases} \frac{n_{XY}(\pi_N[z])}{n_X(\pi_N[z]) \mu_Y(\pi_N[z]_Y)}, & z \in \bar{\mathcal{Z}}_N, \\ 0, & \text{otherwise.} \end{cases} \quad (7)$$

We assume that $\delta_N \downarrow 0$ and that the truncation captures asymptotically all the probability mass, i.e.,

$$\mathbb{P}_{XY}(Y \notin \bar{\mathcal{Y}}_N) \rightarrow 0 \quad \text{almost surely as } N \rightarrow \infty.$$

We assume a deterministic boundary convention (e.g., half-open intervals) so that partition cells from a disjoint cover up to μ_Y -null cells.

For a fixed x , the map $y \mapsto \hat{f}_{\pi_N}(x, y)$ is piecewise constant over the sets $\{A_Y : A \in \pi_N, x \in A_X\}$, and its normalizing factor depends on the corresponding X -projections A_X . Unless these sets form a partition of $\bar{\mathcal{Y}}_N$ with a common denominator, $\hat{f}_{\pi_N}(x, \cdot)$ need not integrate to one. When a proper conditional density on $\bar{\mathcal{Y}}_N$ is required, we therefore use the normalized version

$$\bar{f}_{\pi_N}(x, y) = \frac{\hat{f}_{\pi_N}(x, y)}{\int_{\bar{\mathcal{Y}}_N} \hat{f}_{\pi_N}(x, y') d\mu_Y(y')}, \quad (8)$$

whenever the denominator is positive.

The next section describes how to efficiently choose π_N to optimize a conditional log-loss objective.

2.4. Tree Construction Algorithm

We build a data-dependent partition π_N of $\bar{\mathcal{Z}}_N = \mathcal{X} \times \bar{\mathcal{Y}}_N$ using a greedy and best-first tree procedure. Each leaf corresponds to a measurable product cell

$$A = A_X \times A_Y,$$

and the tree encodes a recursive refinement of such cells. Intuitively, splits on X refine regions of the covariate space, while splits on Y refine the outcome bins inside a fixed covariate region. This joint-space partition is exactly what is needed by the estimator (7), since it defines (for each x -region) a data-adaptive histogram on Y , as illustrated in Figure 1.

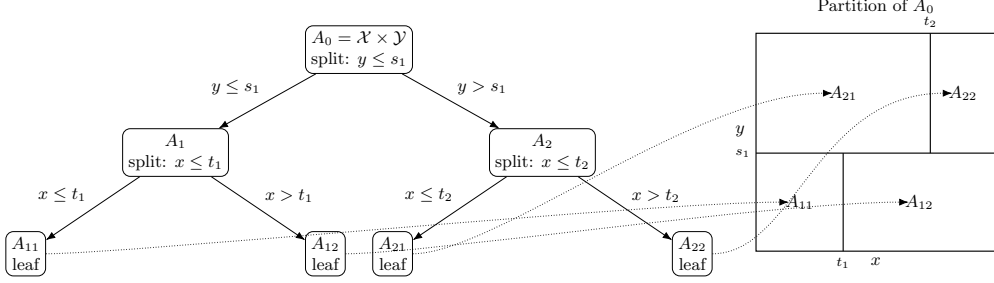


Figure 1. Illustration of a partition of the joint space $Z = X \times Y$. Each leaf of the tree corresponds to a rectangular cell in the induced partition (right). For a fixed query $x = t$, the leaves whose X -projection contains t form a histogram over Y : the associated Y -intervals A_Y are the bins, and the estimator is constant on each bin. In particular, for $x \leq t_1$ the slice $x = t$ intersects two leaves, yielding a two-bin histogram defined by A_{11} and A_{12} ; for $t_1 < x \leq t_2$, it intersects the leaves A_{21} and A_{12} . On each cell, the conditional density is estimated from empirical counts normalized by the Y -volume $\mu_Y(A_Y)$.

2.4.1. CANDIDATE SPLITS AND FEASIBILITY

A candidate split acts on a single coordinate of $Z = (X, Y)$ and preserves the product structure of the leaves:

$$A \longrightarrow \{A_l, A_r\}, \quad A = A_l \uplus A_r \\ A_l = A_{l,X} \times A_{l,Y}, \quad A_r = A_{r,X} \times A_{r,Y}.$$

If we split along an X -coordinate, then $A_{l,Y} = A_{r,Y} = A_Y$ and A_X is partitioned into $A_{l,X} \uplus A_{r,X}$. If we split along a Y -coordinate, then $A_{l,X} = A_{r,X} = A_X$ and A_Y is partitioned into $A_{l,Y} \uplus A_{r,Y}$.

For continuous coordinates $z_\ell \in \mathbb{R}$, we use threshold splits $z_\ell \leq t$ vs. $z_\ell > t$. For categorical coordinates $z_\ell \in \Sigma$, we use subset tests $z_\ell \in S$ vs. $z_\ell \notin S$ for $\emptyset \subsetneq S \subseteq \Sigma$. We only accept splits that keep both children well-defined for the density estimator, i.e.,

$$n_X(A_l) > 0, \quad n_X(A_r) > 0, \\ \mu_Y(A_{l,Y}) > 0, \quad \mu_Y(A_{r,Y}) > 0.$$

Clearly, when splitting on a Y -coordinate, $n_X(A_l) = n_X(A_r) = n_X(A)$.

Candidate splits producing a child with $n_X(A) = 0$ or $\mu_Y(A_Y) = 0$ are discarded; if no admissible split exists for a leaf, it is declared terminal.

2.4.2. LOG-LOSS OBJECTIVE AND SPLIT GAIN

Given a partition π , recall that the piecewise-constant conditional density estimate is $f_\pi(z) = \mathbb{P}_{XY}(\pi[z])/\nu(\pi[z])$ with $\nu = \mathbb{P}_X \otimes \mu_Y$. We score a partition using the conditional negative log-likelihood

$$\mathcal{L}(\pi) := -\mathbb{E}_{\mathbb{P}_{XY}} [\log f_\pi(Z)] \quad (9) \\ = -\sum_{A \in \pi} \mathbb{P}_{XY}(A) \log \left(\frac{\mathbb{P}_{XY}(A)}{\mathbb{P}_X(A_X) \mu_Y(A_Y)} \right),$$

with conventions $0 \log 0 := 0$.

Consider splitting a leaf $A \in \pi$ into A_l, A_r and let $\pi' := (\pi \setminus \{A\}) \cup \{A_l, A_r\}$. The population gain is the log-loss reduction

$$G(\pi', \pi) := \mathcal{L}(\pi) - \mathcal{L}(\pi') \geq 0,$$

and can be written as a Jensen gap (Appendix A).

In practice, we maximize the empirical gain obtained by replacing \mathbb{P}_{XY} and \mathbb{P}_X with their empirical counterparts.

$$\widehat{G}(\pi', \pi) = \frac{n_{XY}(A_l)}{N} \log \left(\frac{n_{XY}(A_l)}{n_X(A_l) \mu_Y(A_{l,Y})} \right) \\ + \frac{n_{XY}(A_r)}{N} \log \left(\frac{n_{XY}(A_r)}{n_X(A_r) \mu_Y(A_{r,Y})} \right) \\ - \frac{n_{XY}(A)}{N} \log \left(\frac{n_{XY}(A)}{n_X(A) \mu_Y(A_Y)} \right), \quad (10)$$

where any term with $n_{XY}(\cdot) = 0$ contributes 0.

2.4.3. BEST-FIRST GROWTH WITH EXPLOITATION AND OPTIONAL EXPLORATION BUDGETS

The tree is grown by repeatedly selecting a leaf and splitting it, under a global split budget k_N . Our default procedure is *gain-based* (exploitation), which greedily chooses the split that maximizes the empirical log-loss gain (10). For worst-case $L^1(\nu)$ -consistency guarantees (Section 3), we also analyze a *hybrid* variant that injects a small number of geometry-driven splits (exploration) to enforce leaf shrinkage.

Exploitation (gain-based) step. For each current leaf A , we search over admissible one-coordinate splits and record the best achievable empirical gain. We then split the leaf–split pair with the largest gain among all leaves. Operationally, we maintain a priority queue of leaves by their current best gain; after splitting a leaf, only that leaf’s entry needs to be recomputed.

Optional exploration (diameter-based) step. Pure gain maximization can, in principle, stall on coarse partitions when all

one-step gains are zero, even though f varies within the leaf (for a standard greedy-tree failure mode, see (Rosell et al., 2005)). To obtain a worst-case leaf-shrinkage condition (used in Section 3), the hybrid variant allocates an exploration budget $k_{N,e}$ and repeatedly splits the *populated* leaf (i.e., with $n_{XY}(A) > 0$) of the largest diameter. The split coordinate is chosen as the one with the largest side length inside that leaf. For bounded continuous sides, we split at the geometric mean value within the leaf; for categorical coordinates, we split off a (random) singleton category. If the selected leaf is unbounded along the chosen continuous coordinate, we instead split at an empirical threshold so that all samples in the leaf fall into a bounded child (e.g., at $\max\{z_i : z_i \in A\}$, creating one bounded populated child and one empty unbounded remainder). We design the exploration splits so that each such split satisfies a uniform diameter contraction

$$\max(\text{diam}(A_l), \text{diam}(A_r)) \leq \rho \text{diam}(A)$$

for some $\rho \in [1/2, 1]$, as required by the consistency analysis in Section 3. One simple schedule is to perform the $k_{N,e}$ exploration splits first and then use the remaining $k_N - k_{N,e}$ steps for gain-based refinement; interleaving the two phases is also possible. The asymptotic scaling conditions on k_N and $k_{N,e}$ required for consistency are explicitly stated in Section 3.

2.4.4. EFFICIENT SPLIT SEARCH AND COMPLEXITY

A computational advantage of (10) is that it depends only on simple count statistics for candidate children. For a continuous coordinate z_ℓ and a leaf A , candidate thresholds are the midpoints between consecutive distinct values observed in the leaf. After sorting the relevant values within each leaf, we scan thresholds in increasing order and update the required counts using prefix sums, enabling evaluation of all thresholds on that coordinate in linear time, plus sorting. Algorithm 1 in Section B.1 gives one concrete implementation using two sorted index lists: one for the covariate samples in A_X (to update n_X when splitting on X), and another for the joint samples in A (to update n_{XY} and to handle splits on either X or Y).

For categorical coordinates with alphabet Σ , we avoid enumerating all $2^{|\Sigma|} - 2$ subset tests by computing per-category count statistics inside the leaf, sorting categories by the score, and scanning the $|\Sigma| - 1$ prefix thresholds. Section B.2 shows that this scan attains the best subset split for a leaf and coordinate.

Let d_Z be the number of splittable coordinates in $Z = (X, Y)$. With per-leaf sorting, evaluating all candidate splits at a leaf with $n_X(A)$ covariate points costs $O(d_Z n_X(A) \log n_X(A))$ in a straightforward implementation.

For categorical coordinates, since alphabet sizes are fixed, the sort-and-scan subset search adds only $O(n_X(A))$ work per leaf, which is smaller than the split search cost over continuous coordinates. Summed over the best-first growth, this leads to an overall time complexity on the order of $O(d_Z N \log N)$ with global presorting and maintained sorted indices, or $O(d_Z N \log^2 N)$ when sorting within each node for balanced trees, matching the scaling observed in practice for CART trees.

2.5. Partition Forest (bagging ensemble)

To improve predictive stability and log-loss, we also consider an ensemble variant, *Partition Forest*, obtained by bagging *Partition Trees*. We fit B trees independently, where tree b is trained on a bootstrap sample $\mathcal{D}^{(b)}$ (and optionally using random feature subsampling at each split, as in Random Forests (Breiman, 2001)). Given per-tree conditional density estimates $\{\hat{f}_{\pi_N}^{(b)}\}_{b=1}^B$, the forest predictor is the averaged density

$$\hat{f}_{\pi_N}^F(x, y) := \frac{1}{B} \sum_{b=1}^B \hat{f}_{\pi_N}^{(b)}(x, y),$$

which is then normalized as in Equation (8) to obtain $\bar{f}_{\pi_N}^F(x, y)$.

3. Consistency

This section provides sufficient conditions for $L^1(\nu)$ -consistency of the piecewise-constant estimator when the underlying data-dependent partition satisfies standard complexity and shrinkage requirements. To guarantee shrinkage under arbitrary distributions, we analyze a *hybrid* tree construction that injects a vanishing fraction of diameter-reducing splits.

The consistency of data-driven partitions for joint density estimation has been studied by (Lugosi & Nobel, 1996). Here, we adapt their results to conditional density estimates and provide sufficient conditions for them. Let the maximum cell count of a family of partitions \mathcal{A} :

$$m(\mathcal{A}) = \sup_{\pi \in \mathcal{A}} |\pi|$$

And the maximum cell count on the \mathcal{X} domain:

$$m_X(\mathcal{A}_N) := \sup_{\pi \in \mathcal{A}_N} |\{A_X : A \in \pi\}|. \quad (11)$$

Denote by $\Delta(\mathcal{A}, \mathcal{D})$ the number of distinct partitions of the finite set \mathcal{D} induced by partitions in \mathcal{A} . Define the growth function $\Delta_N^*(\mathcal{A})$ as:

$$\Delta_N^*(\mathcal{A}) := \max_{\mathcal{D} \in \mathcal{Z}^N} \Delta(\mathcal{A}, \mathcal{D})$$

Finite VC dimension of X -leaf projections. We assume that the class of X -projections of leaves has finite VC dimension. In our implementation, it consists of axis-aligned rectangles in $\mathbb{R}^{d_{x,c}}$ times categorical cylinder sets over finite alphabets. This class has a finite VC dimension by standard results on VC bounds for rectangles and finite product classes (Van Der Vaart & Wellner, 2009).

Theorem 3.1 describes the sufficient conditions for the data-driven partitions of \mathcal{Z} to be $L^1(\nu)$ -consistent.

The following results analyze the idealized tree construction without finite-sampling pruning or leaf-size constraints, and the consistency of the normalized estimator used in practice follows from Corollary C.7.

Theorem 3.1. *Let $\mathcal{D}_N = \{(X_i, Y_i)\}_{i=1}^N = \{\mathcal{Z}_i\}_{i=1}^N$ be a set of observations belonging to $\mathcal{Z} := \mathcal{X} \times \mathcal{Y}$ with joint distribution $\mathbb{P}_{XY} \ll \nu$. Consider $\bar{\mathcal{Y}}_N$ a ν -measurable truncation of \mathcal{Y} as in Equation (6). Let $\Pi = \{\pi_1, \dots, \pi_N\}$ be a partitioning scheme for $\bar{\mathcal{Z}}_N := \mathcal{X} \times \bar{\mathcal{Y}}_N$, and let \mathcal{A}_N be the collection of partitions associated with the rule π_N . Denote by $f(X, Y)$ the conditional density of Y given X and the estimate as in Equation (7). Assume:*

1. $N^{-1}m(\mathcal{A}_N) \xrightarrow{N \rightarrow \infty} 0$
2. $N^{-1} \log \Delta_N^*(\mathcal{A}_N) \xrightarrow{N \rightarrow \infty} 0$
3. There exists a sequence $\gamma_N \xrightarrow{N \rightarrow \infty} 0$ such that $\mathbb{P}_{XY}(\{z \in \bar{\mathcal{Z}}_N : \text{diam}(\pi_N[z]) > \gamma_N\}) \xrightarrow{N \rightarrow \infty} 0$
4. $m_X(\mathcal{A}_N) \sqrt{\frac{\log N}{N}} \rightarrow 0$.

Then

$$\|\hat{f}_{\pi_N} - f\|_{L^1(\nu)} \rightarrow 0 \quad \text{as } N \rightarrow \infty,$$

almost surely.

Proof. See Appendix C for the proof. \square

Theorem 3.2 describes the sufficient conditions for consistency of the tree algorithm when augmented with exploration splits.

Theorem 3.2. *(Consistency of the hybrid tree conditional density estimator) Let \hat{f}_{π_N} be the tree estimator in (7), built from a best-first greedy construction that (i) uses the empirical log-loss gain (10) for its main split selection, and (ii) additionally allocates an exploration budget $k_{N,e}$ that always splits the current largest leaf.*

Assume:

1. The total split budget satisfies $k_N = o(\sqrt{\frac{N}{\log N}})$ and $k_N \rightarrow \infty$. (e.g. $\sqrt[6]{N}$, $a > 2$), and the exploration budget $k_{N,e}$ satisfies $0 \leq k_{N,e} \leq k_N$ and $k_{N,e} \rightarrow \infty$.
2. (Per-split contraction for exploration) Every exploration split $A \rightarrow \{A_l, A_r\}$ satisfies $\max(\text{diam}(A_l), \text{diam}(A_r)) \leq \rho \text{diam}(A)$ for some $\rho \in [1/2, 1]$.

Then

$$\|\hat{f}_{\pi_N} - f\|_{L^1(\nu)} \rightarrow 0 \quad \text{as } N \rightarrow \infty,$$

almost surely.

Proof sketch. The argument consists in verifying the assumptions of Theorem 3.1. With k_N splits, Lemma C.4 establishes conditions 1, 2, and 4. Condition 3 follows from the exploration rule, which ensures sufficient visitation while vanishing asymptotically, provided that $k_{N,e} = o(\sqrt{N/\log N})$ and $k_{N,e} \rightarrow \infty$. A complete proof is given in Appendix C. \square

The split budget can be defined through hyperparameters. The next corollary extrapolates Theorem 3.1 to the normalized counterpart \bar{f}_{π_N} .

Corollary 3.3. *Consider the setting in Theorem 3.1 and the definition of \bar{f}_{π_N} as in Equation (8). Then*

$$\|\bar{f}_{\pi_N} - f\|_{L^1(\nu)} \rightarrow 0 \quad \text{as } N \rightarrow \infty,$$

almost surely.

Proof. See Appendix C.5 for the proof. \square

4. Experiments

We conduct experiments to answer the following questions:

- (1) How does the proposed algorithm compare with respect to the traditional CART decision tree and its probabilistic variants?
- (2) Can the proposed tree handle both homoscedastic and heteroscedastic noise?
- (3) Can the proposed tree algorithm correctly ignore irrelevant or noisy features?

Our experiments assess the performance of the proposed greedy gain-based splitting strategy on both classification and regression tasks. We focus on comparisons against the CART decision tree algorithm (Breiman et al., 2017), implemented in scikit-learn (Pedregosa et al., 2011). Additionally, we evaluate classical ensemble methods based on decision trees, including Random Forest (Pedregosa et al., 2011) and XGBoost (Chen, 2016).

We use five-fold cross-validation, with a nested train-validation split within each fold for hyperparameter tuning. Hyperparameter tuning is performed using Optuna (Akiba et al., 2019), with a budget of 200 trials and a time limit of 20 minutes per model. For CDTree, hyperparameters are not tuned, following the recommendations of the original implementation. Model selection is based on log-loss evaluated on the validation data. Additional details regarding hyperparameters and experimental settings are provided in Appendix D. All experiments were conducted using our implementation of *Partition Trees* and *Partition Forests* available at github.com/felipeangelimvieira/partition_tree.

4.1. Classification

Table 1 describes the log-loss obtained by Partition Tree and Partition Forest in comparison with their respective baselines. Among non-ensemble methods, Partition Trees outperform CART trees on the majority of datasets (8 out of 9). For ensemble methods, Partition Forest achieves superior probabilistic classification performance than Random Forest, a bagging-based ensemble of CART trees, on most datasets. Overall, XGBoost achieves the strongest performance on this task, achieving the lowest average rank (1.44) and consistently outperforming both bagging-based approaches (Random Forest and Partition Forest).

Table 1. Log-loss results over 5-fold cross-validation for ensemble and non-ensemble tree methods on classification tasks (mean \pm std). Lower is better. Best for ensemble and non-ensemble in bold. The last row represents the average ranking of each method in its group. *Underline* indicates statistical ties according to a paired t-test at the 5% significance level (run separately within ensemble and non-ensemble groups)

	Non-ensemble models		Ensemble models			
	CART	Partition Tree	Partition Forest	Random Forest	NGBoost	XGBoost
iris	<i>0.70 \pm 0.53</i>	0.46 \pm 0.38	<i>0.50 \pm 0.43</i>	<i>0.35 \pm 0.51</i>	<i>0.46 \pm 0.40</i>	0.19 \pm 0.11
breast	<i>1.07 \pm 0.81</i>	0.64 \pm 0.05	<i>0.58 \pm 0.02</i>	0.55 \pm 0.05	<i>0.56 \pm 0.05</i>	<i>0.57 \pm 0.03</i>
wine	<i>1.26 \pm 0.30</i>	1.02 \pm 0.06	0.86 \pm 0.04	<i>0.89 \pm 0.11</i>	1.00 \pm 0.04	0.93 \pm 0.04
digits	1.59 \pm 0.28	0.45 \pm 0.04	0.29 \pm 0.01	0.30 \pm 0.01	0.44 \pm 0.07	0.11 \pm 0.02
spam	<i>0.32 \pm 0.14</i>	0.22 \pm 0.04	0.17 \pm 0.03	<i>0.18 \pm 0.04</i>	0.19 \pm 0.03	0.14 \pm 0.03
support2	<i>0.28 \pm 0.04</i>	0.28 \pm 0.02	<i>0.24 \pm 0.02</i>	<i>0.27 \pm 0.06</i>	0.24 \pm 0.02	0.23 \pm 0.01
letter	1.43 \pm 0.08	0.62 \pm 0.17	0.50 \pm 0.02	0.28 \pm 0.01	0.96 \pm 0.29	0.17 \pm 0.02
bank	0.23 \pm 0.01	0.22 \pm 0.01	0.20 \pm 0.01	0.20 \pm 0.01	0.22 \pm 0.01	0.20 \pm 0.01
adult	0.92 \pm 0.01	0.93 \pm 0.01	0.90 \pm 0.01	0.90 \pm 0.00	0.91 \pm 0.00	0.88 \pm 0.00
Avg. rank	1.89	1.11	2.44	2.56	3.56	1.44

4.2. Regression Task

We compare *Partition Trees* against trees probabilistic regressions: CDTree (Yang & van Leeuwen, 2024), CADET (Cousins & Riondato, 2019), and NGBoost (Duan et al., 2020). Since CART decision trees do not natively support probabilistic regression, we adopt the residual-based approach implemented in `skpro` (Gressmann et al., 2018) for CART, XGBoost, and Random Forest. It assumes normally distributed residuals and estimates predictive variance using an inner train-test split.

The log-loss results are summarized in Table 2. Among non-ensemble methods, CDTree achieves the best average ranking. However, its high computational complexity limits scalability and makes integration into ensemble frameworks impractical (see the runtime comparison in Appendix E and Figure 4). Comparing *Partition Trees* with CADET, our method outperforms CADET on four of the six largest datasets (i.e., Air, Power, California, and Protein). This suggests that Partition Tree may benefit from larger sample sizes than the parametric baseline. For ensemble methods, *Partition Forests* outperform Random Forests on most datasets (8 out of 10) and achieve performance competitive with NGBoost, which achieves the best overall ranking. These results indicate that *Partition Forests* are substantially better suited for probabilistic regression tasks than their CART-based counterparts. Additional results for the root mean squared error (RMSE) and predictive standard deviations are provided in Section D.3.

Table 2. Log-loss results over 5-fold cross-validation for ensemble and non-ensemble tree methods on regression tasks. Best for each group in bold (lower is better). Datasets are ordered by size. *Underline* indicates statistical ties according to a paired t-test at the 5% significance level (run separately within ensemble and non-ensemble groups)

	Non-ensemble models				Ensemble models			
	Partition Tree	CART	CADET	CDTree	Partition Forest	Random Forest	NGBoost	XGBoost
diabetes	<u>5.65</u>	17.93	<u>5.59</u>	5.58	5.49	14.21	<u>5.50</u>	16.81
boston	<u>2.90</u>	8.39	<u>2.89</u>	2.88	2.53	4.60	<u>2.59</u>	4.60
energy	2.36	<u>1.67</u>	<u>10.81</u>	1.55	2.06	1.55	0.60	1.53
concrete	<u>3.70</u>	7.45	3.52	<u>3.66</u>	3.36	3.86	3.11	<u>3.44</u>
kin8nm	<u>-0.18</u>	9.42	-0.22	<u>-0.18</u>	<u>-0.45</u>	3.30	-0.49	2.05
air	<u>2.12</u>	13.49	<u>13.78</u>	6.42	2.02	11.35	5.62	12.25
power	<u>2.87</u>	3.13	<u>2.90</u>	2.93	<u>2.60</u>	2.63	2.77	2.59
naval	-4.38	4.69	-4.78	-4.29	-4.72	-4.98	-5.05	-4.93
california	0.69	7.07	0.88	0.58	0.42	3.11	0.52	2.51
protein	2.22	12.31	3.13	2.18	2.10	6.19	2.79	7.23
Avg. rank	2.30	3.70	2.30	1.70	1.90	3.30	1.80	3.00

4.2.1. ROBUSTNESS AGAINST NOISE AND REDUNDANT FEATURES

To evaluate robustness to correlated and redundant features, we augment the feature matrix $X \in \mathbb{R}^{N \times n_x}$ with k additional noisy columns. Each added feature is generated by copying a randomly selected original column X_{c_i} and adding Gaussian noise $\epsilon \sim \mathcal{N}(0, \sigma_i^2)$. The noise scale is set to the mean absolute value of the selected column, $\sigma_i = \frac{1}{N} \sum_j |X_{j,c_i}|$, which ensures that the perturbation is proportional to the feature's magnitude while preserving substantial correlation with the original predictor.

We evaluated robustness using the Concrete Compressive Strength dataset using five-fold cross-validation. The results are summarized in Figure 2. CDTree maintains a stable negative log-likelihood as the number of features increases, indicating robustness to correlated feature duplication. In contrast, Partition Tree showed a gradual degradation in the

negative log-likelihood, although its performance variance across folds remains lower than that of CADET. This suggests that while Partition Tree is less robust in expectation, it yields more consistent predictions under feature corruption.

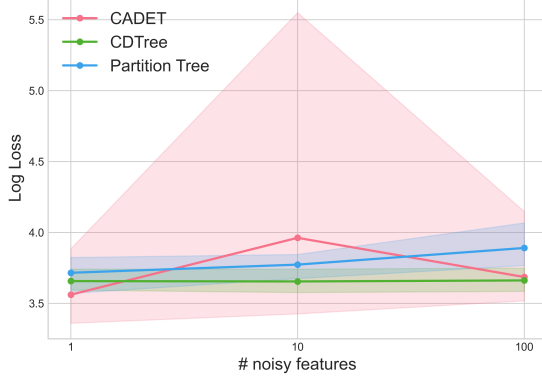


Figure 2. Negative log-likelihood of probabilistic tree models on the Concrete Compressive Strength dataset. As the number of noisy features increases, the models exhibit different sensitivity patterns. Shaded bands denote the minimum and maximum values across five cross-validation folds.

4.2.2. HOMOSCEDASTIC AND HETEROSCEDASTIC NOISE

We study robustness to label noise by constructing semi-synthetic datasets in which we perturb the target values. For the homoscedastic setting, we add Gaussian noise with standard deviation $\sigma(\lambda) = \lambda \cdot \frac{1}{N} \sum_i |y_i|$, with $\lambda \in \{0.1, 0.5, 1.0, 1.5\}$. For the heteroscedastic case, we add a sample-dependent Gaussian noise with $\sigma_i(\lambda) = \lambda |y_i|$, using the same values of λ . Figure 3 shows that Partition Tree degrades with noise at a rate comparable to CDTree in both settings, while CADET exhibits higher variability across folds.

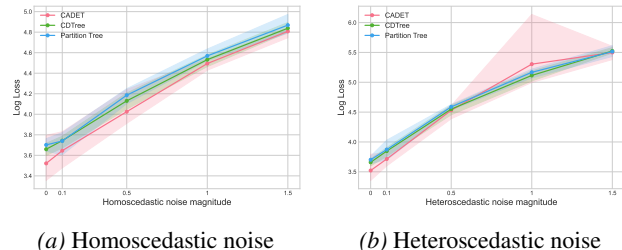


Figure 3. Performance of probabilistic tree models under increasing label-noise magnitude on the Concrete Compressive Strength dataset. Shaded bands indicate the minimum and maximum negative log-likelihood across five cross-validation folds.

5. Conclusion

We introduced Partition Trees, a decision-tree framework for conditional density estimation over general outcome

spaces, including continuous, categorical, and mixed-type targets. The method is grounded in a measure-theoretic formulation in which conditional densities are defined as a Radon-Nikodym derivative with respect to the dominating measure $\mathbb{P}_X \otimes \mu_Y$. This yields a unified piecewise-constant estimator that naturally covers both classification and regression within a single framework.

Partition Trees are learned via a greedy, best-first procedure that directly optimizes a conditional log-loss objective on data-adaptive partitions of the joint covariate-outcome space. We further analyzed a hybrid variant that interleaves a vanishing fraction of diameter-reducing exploration splits, and showed that it admits an $L^1(\nu)$ -consistency guarantee under standard partition growth and shrinkage conditions. An ensemble extension, *Partition Forests*, averages conditional densities across trees and improves predictive stability and log-loss performance.

Empirically, the proposed models demonstrate competitive probabilistic performance across a diverse set of classification and regression benchmarks. *Partition Forests* typically achieve lower log-loss than CART-based trees and often improve over Random Forests, while providing accurate predictive densities and competitive point predictions in regression tasks. Experiments also highlight robustness to heteroscedastic noise and redundant features.

Several directions for future work remain open. From an algorithmic perspective, integrating *Partition Forests* into boosting frameworks and developing pruning strategies tailored to conditional density objectives may further improve efficiency performance and efficiency. More broadly, *Partition Trees*' ability to handle heterogeneous and mixed-type outcomes makes them a natural candidate for integration into causal inference pipelines, where flexible conditional density estimation plays a central role.

Acknowledgments

This research was partially funded by the French National Research Agency (ANR) under Grant No. ANR-23-CPJ1-0099-01.

References

Akiba, T., Sano, S., Yanase, T., Ohta, T., and Koyama, M. Optuna: A next-generation hyperparameter optimization framework. In *25th ACM SIGKDD International Conference on Knowledge Discovery & Data Mining*, pp. 2623–2631, 2019.

Alpaydin, E. and Kaynak, C. Optical Recognition of Handwritten Digits. UCI Machine Learning Repository, 1998. DOI: <https://doi.org/10.24432/C50P49>.

Breiman, L. Random forests. *Machine learning*, 45(1): 5–32, 2001.

Breiman, L., Friedman, J., Olshen, R. A., and Stone, C. J. *Classification and regression trees*. Chapman and Hall/CRC, 2017.

Chen, T. XGBoost: A scalable tree boosting system. *Cornell University*, 2016.

Coraddu, A., Oneto, L., Ghio, A., Savio, S., Anguita, D., and Figari, M. Machine learning approaches for improving condition-based maintenance of naval propulsion plants. *Proceedings of the Institution of Mechanical Engineers, Part M: Journal of Engineering for the Maritime Environment*, 230(1):136–153, 2016.

Corke, P. I. A robotics toolbox for matlab. *IEEE Robotics & Automation Magazine*, 3(1):24–32, 2002.

Cortez, P., Cerdeira, A., Almeida, F., Matos, T., and Reis, J. Modeling wine preferences by data mining from physicochemical properties. *Decision support systems*, 47(4): 547–553, 2009.

Cousins, C. and Riondato, M. CaDET: interpretable parametric conditional density estimation with decision trees and forests. *Machine Learning*, 108(8):1613–1634, 2019.

De Vito, S., Massera, E., Piga, M., Martinotto, L., and Di Francia, G. On field calibration of an electronic nose for benzene estimation in an urban pollution monitoring scenario. *Sensors and Actuators B: Chemical*, 129(2): 750–757, 2008.

Duan, T., Anand, A., Ding, D. Y., Thai, K. K., Basu, S., Ng, A., and Schuler, A. Ngboost: Natural gradient boosting for probabilistic prediction. In *International Conference on Machine Learning*, pp. 2690–2700. PMLR, 2020.

Fisher, R. A. The use of multiple measurements in taxonomic problems. *Annals of eugenics*, 7(2):179–188, 1936.

Fisher, W. D. On grouping for maximum homogeneity. *Journal of the American Statistical Association*, 53(284): 789–798, 1958.

Frey, P. W. and Slate, D. J. Letter recognition using holland-style adaptive classifiers. *Machine learning*, 6(2):161–182, 1991.

Gressmann, F. and Kiraly, F. skpro: A domain-agnostic modelling framework for probabilistic supervised learning. In *Machine Learning Open Source Software*, 2018.

Gressmann, F., Király, F. J., Mateen, B., and Oberhauser, H. Probabilistic supervised learning. *arXiv:1801.00753*, 2018.

Harrell Jr, F. E. and Harrell Jr, M. F. E. Package ‘hmisc’. *CRAN2018*, 2019:235–236, 2019.

Harrison Jr, D. and Rubinfeld, D. L. Hedonic housing prices and the demand for clean air. *Journal of Environmental Economics and Management*, 5(1):81–102, 1978.

Hopkins, M., Reeber, E., Forman, G., and Suermontd, J. Spambase. UCI Machine Learning Repository, 1999. DOI: <https://doi.org/10.24432/C53G6X>.

Kahn, M. Diabetes. UCI Machine Learning Repository, 1994. DOI: <https://doi.org/10.24432/C5T59G>.

Kass, G. V. An exploratory technique for investigating large quantities of categorical data. *Journal of the Royal Statistical Society: Series C (Applied Statistics)*, 29(2): 119–127, 1980.

Kohavi, R. and Becker, B. Adult data set. *UCI machine learning repository*, 5:2093, 1996.

Loh, W.-Y. Fifty years of classification and regression trees. *International Statistical Review*, 82(3):329–348, 2014.

Lugosi, G. and Nobel, A. Consistency of data-driven histogram methods for density estimation and classification. *The Annals of Statistics*, 24(2):687–706, 1996.

Morgan, J. N. and Sonquist, J. A. Problems in the analysis of survey data, and a proposal. *Journal of the American Statistical Association*, 58(302):415–434, 1963.

Moro, S., Cortez, P., and Rita, P. A data-driven approach to predict the success of bank telemarketing. *Decision Support Systems*, 62:22–31, 2014.

Pace, R. K. and Barry, R. Sparse spatial autoregressions. *Statistics & Probability Letters*, 33(3):291–297, 1997.

Pedregosa, F., Varoquaux, G., Gramfort, A., Michel, V., Thirion, B., Grisel, O., Blondel, M., Prettenhofer, P., Weiss, R., Dubourg, V., Vanderplas, J., Passos, A., Cournapeau, D., Brucher, M., Perrot, M., and Duchesnay, E. Scikit-learn: Machine learning in Python. *Journal of Machine Learning Research*, 12:2825–2830, 2011.

Rana, P. Physicochemical Properties of Protein Tertiary Structure. UCI Machine Learning Repository, 2013. DOI: <https://doi.org/10.24432/C5QW3H>.

Rosell, B., Hellerstein, L., Ray, S., and Page, D. Why skewing works: Learning difficult boolean functions with greedy tree learners. In *22nd International Conference on Machine Learning*, pp. 728–735, 2005.

Tsanas, A. and Xifara, A. Accurate quantitative estimation of energy performance of residential buildings using statistical machine learning tools. *Energy and buildings*, 49: 560–567, 2012.

Tüfekci, P. Prediction of full load electrical power output of a base load operated combined cycle power plant using machine learning methods. *International Journal of Electrical Power & Energy Systems*, 60:126–140, 2014.

Van Der Vaart, A. and Wellner, J. A. A note on bounds for vc dimensions. *Institute of Mathematical Statistics collections*, 5:103, 2009.

Yang, L. and van Leeuwen, M. Conditional density estimation with histogram trees. *Advances in Neural Information Processing Systems*, 37:117315–117339, 2024.

Yeh, I.-C. Modeling of strength of high-performance concrete using artificial neural networks. *Cement and Concrete Research*, 28(12):1797–1808, 1998.

Zwitter, M. and Soklic, M. Breast Cancer. UCI Machine Learning Repository, 1988. DOI: <https://doi.org/10.24432/C51P4M>.

A. Properties of the Log-loss Gain

We first show that the population gain of a candidate split is a Jensen gap, related to child averages. Define $\varphi(u) = u \log u$. For a leaf $A \in \pi$ and split $A \rightarrow \{A_l, A_r\}$. Let π' be the partition after splitting A . The population loss of a partition π can be expressed as:

$$\mathcal{L}(\pi) = -\mathbb{E}_{\mathbb{P}_{XY}}[\log f_\pi] = -\mathbb{E}_\nu[f_\pi \log f_\pi]$$

so the population gain can also be written:

$$G(\pi', \pi) = G(\{A_l, A_r\}, \{A\}) \tag{12}$$

$$= \nu(A_l)\varphi(c_{A_l}) + \nu(A_r)\varphi(c_{A_r}) - \nu(A)\varphi(c_A) \tag{13}$$

$$= \left(\frac{\nu(A_l)}{\nu(A)}\varphi(c_{A_l}) + \frac{\nu(A_r)}{\nu(A)}\varphi(c_{A_r}) - \varphi(c_A) \right) \nu(A) \tag{14}$$

where $c_A = \frac{1}{\nu(A)} \int_A f d\nu$.

From this identity, we derive the following proposition: the gain is a Jensen Gap.

Proposition A.1 (Population gain is a Jensen Gap). *Consider a cell A and two children A_l and A_r , $A = A_l \cup A_r$. Let $\nu_A = \nu(\cdot \cap A)/\nu(A)$ be a normalized restriction of the measure ν to A and let $\mathcal{G} := \sigma(\{A_l, A_r\})$ be the σ -algebra generated by the split. Assume $\nu(A), \nu(A_l), \nu(A_r) > 0$. The gain can be expressed by the following Jensen gap times the measure $\nu(A)$:*

$$G(\pi', \pi) = (\mathbb{E}_{\nu_A}[\varphi(X)] - \varphi(\mathbb{E}_{\nu_A}[X])) \cdot \nu(A)$$

with $X(z) = \mathbb{E}_{\nu_A}[f \mid \mathcal{G}](z)$, $z \sim \nu_A$.

Proof. Define the normalized restriction $\nu_A(B) := \nu(B \cap A)/\nu(A)$ for measurable B . Then

$$c_A = \frac{1}{\nu(A)} \int_A f d\nu = \int_A f d\nu_A = \mathbb{E}_{\nu_A}[f].$$

Let $\mathcal{G} := \sigma(\{A_l, A_r\})$. Since \mathcal{G} has atoms A_l and A_r , the conditional expectation $X(z) := \mathbb{E}_{\nu_A}[f \mid \mathcal{G}](z)$ is \mathcal{G} -measurable, hence constant on each child: $X = u_l \mathbf{1}_{A_l} + u_r \mathbf{1}_{A_r}$. By the defining property of conditional expectation, for $B \in \{A_l, A_r\}$,

$$\int_B X d\nu_A = \int_B f d\nu_A.$$

Thus $u_l = \frac{1}{\nu_A(A_l)} \int_{A_l} f d\nu_A = \frac{1}{\nu(A_l)} \int_{A_l} f d\nu = c_{A_l}$ and similarly $u_r = c_{A_r}$. Therefore, ν_A -a.e.,

$$X(z) = \mathbb{E}_{\nu_A}[f \mid \mathcal{G}](z) = \begin{cases} c_{A_l}, & z \in A_l, \\ c_{A_r}, & z \in A_r. \end{cases}$$

Let $w := \nu_A(A_l) = \nu(A_l)/\nu(A)$. Then

$$\mathbb{E}_{\nu_A}[\varphi(X)] = w \varphi(c_{A_l}) + (1 - w) \varphi(c_{A_r}) = \frac{\nu(A_l)}{\nu(A)} \varphi(c_{A_l}) + \frac{\nu(A_r)}{\nu(A)} \varphi(c_{A_r}).$$

Also, by the tower property,

$$\mathbb{E}_{\nu_A}[X] = \mathbb{E}_{\nu_A}[\mathbb{E}_{\nu_A}[f \mid \mathcal{G}]] = \mathbb{E}_{\nu_A}[f] = c_A.$$

Plugging these identities into (12) yields

$$G(\pi', \pi) = \nu(A) \left(\mathbb{E}_{\nu_A}[\varphi(X)] - \varphi(\mathbb{E}_{\nu_A}[X]) \right),$$

as claimed. \square

Since the gain is a Jensen Gap, it is immediate that the gain is always greater than or equal to zero.

Corollary A.2 (Non-negativity of the gain). *For any split $\{A\} \rightarrow \{A_l, A_r\}$, if $\nu(A), \nu(A_l), \nu(A_r) > 0$, then $G(\{A_l, A_r\}, \{A\}) \geq 0$.*

Proof. Use the non-negativity of $\nu(A)$ and the non-negativity of the Jensen Gap in Proposition A.1 to see that $G(\pi', \pi) \geq 0$. \square

B. Algorithm

B.1. Continuous Coordinates

Algorithm 1 illustrates how the split search can be executed for continuous variables. The algorithm does not use presorting (storing the sample order for each feature at the root), which could further improve runtime.

Algorithm 1 Find Best Split (Continuous Coordinate z)

```

1: Input: Coordinate values  $z \in \mathbb{R}^N$ , weights  $w \in \mathbb{R}^N$ , node index sets  $I_x$  (points with  $x_i \in A_X$ ),  $I_{xy}$  (points with  $(x_i, y_i) \in A$ ), flag is_X_feature, routine is_valid(t), and access to  $\mu_Y(A_{l,Y})$ ,  $\mu_Y(A_{r,Y})$ .
2: Output: Best gain  $G^*$  and child index sets.
3:  $G^* \leftarrow -\infty$ 
4:  $I_{x,\text{sort}} \leftarrow \text{argsort}(z[I_x])$ ,  $I_{xy,\text{sort}} \leftarrow \text{argsort}(z[I_{xy}])$ 
5:  $I_x^\uparrow \leftarrow I_x[I_{x,\text{sort}}]$ ,  $I_{xy}^\uparrow \leftarrow I_{xy}[I_{xy,\text{sort}}]$ 
6:  $S_x \leftarrow z[I_x^\uparrow]$ ,  $S_{xy} \leftarrow z[I_{xy}^\uparrow]$ 
7:  $W_x \leftarrow \text{cumsum}(w[I_x^\uparrow])$ ,  $W_{xy} \leftarrow \text{cumsum}(w[I_{xy}^\uparrow])$ 
8:  $N_X \leftarrow W_x[-1]$ ,  $N_{XY} \leftarrow W_{xy}[-1]$ 
9: if is_X_feature then
10:    $\mathcal{C} \leftarrow$  midpoints between consecutive distinct values in  $S_x$ 
11: else
12:    $\mathcal{C} \leftarrow$  midpoints between consecutive distinct values in  $S_{xy}$ 
13: end if
14: Initialize pointers  $p_x \leftarrow 0$ ,  $p_{xy} \leftarrow 0$  {upper-bound positions}
15: for threshold  $t \in \mathcal{C}$  in increasing order do
16:   if is_X_feature then
17:     {Advance  $p_x$  to the last index with  $S_x[p_x] \leq t$ }
18:     while  $p_x + 1 < |S_x|$  and  $S_x[p_x + 1] \leq t$  do
19:        $p_x \leftarrow p_x + 1$ 
20:     end while
21:      $n_X(A_l) \leftarrow W_x[p_x]$ ,  $n_X(A_r) \leftarrow N_X - n_X(A_l)$ 
22:   else
23:     {Y-split does not change  $A_X$ }
24:      $n_X(A_l) \leftarrow N_X$ ,  $n_X(A_r) \leftarrow N_X$ 
25:   end if
26:   {Advance  $p_{xy}$  to the last index with  $S_{xy}[p_{xy}] \leq t$ }
27:   while  $p_{xy} + 1 < |S_{xy}|$  and  $S_{xy}[p_{xy} + 1] \leq t$  do
28:      $p_{xy} \leftarrow p_{xy} + 1$ 
29:   end while
30:    $n_{XY}(A_l) \leftarrow W_{xy}[p_{xy}]$ ,  $n_{XY}(A_r) \leftarrow N_{XY} - n_{XY}(A_l)$ 
31:   Compute  $G$  from Eq. (10) using these counts and  $\mu_Y(A_{l,Y})$ ,  $\mu_Y(A_{r,Y})$ .
32:   if is_valid(t) and  $G > G^*$  then
33:      $G^* \leftarrow G$ , store best  $(t^*, p_x^*, p_{xy}^*)$ 
34:   end if
35: end for
36: if is_X_feature then
37:    $I_x^{(l)} \leftarrow I_x^\uparrow[0 : p_x^* + 1]$ ,  $I_x^{(r)} \leftarrow I_x^\uparrow[p_x^* + 1 :]$ 
38: else
39:    $I_x^{(l)} \leftarrow I_x$ ,  $I_x^{(r)} \leftarrow I_x$ 
40: end if
41:  $I_{xy}^{(l)} \leftarrow I_{xy}^\uparrow[0 : p_{xy}^* + 1]$ ,  $I_{xy}^{(r)} \leftarrow I_{xy}^\uparrow[p_{xy}^* + 1 :]$ 
42: Return  $G^*$ ,  $I_x^{(l)}$ ,  $I_x^{(r)}$ ,  $I_{xy}^{(l)}$ ,  $I_{xy}^{(r)}$ 

```

Example (one continuous feature at one node). Suppose a leaf A contains $n_X(A) = 6$ covariate points with one continuous coordinate z (weights $w_i \equiv 1$ for simplicity) and $n_{XY}(A) = 4$ joint points. Let the sorted values inside the node be

$$S_x = (1, 2, 4, 7, 9, 10), \quad S_{xy} = (2, 4, 9, 10).$$

Candidate thresholds are the midpoints between consecutive distinct values in S_x :

$$\mathcal{C} = \left\{ \frac{1+2}{2} = 1.5, \frac{2+4}{2} = 3, \frac{4+7}{2} = 5.5, \frac{7+9}{2} = 8, \frac{9+10}{2} = 9.5 \right\}.$$

Consider $t = 5.5$. The split index in S_x is the last position with value ≤ 5.5 , namely after $(1, 2, 4)$, so

$$n_X(A_l) = 3, \quad n_X(A_r) = 3.$$

Likewise, the split index in S_{xy} is after $(2, 4)$, so

$$n_{XY}(A_l) = 2, \quad n_{XY}(A_r) = 2.$$

Therefore the gain for this candidate is computed by plugging these four counts (and the corresponding $\mu_Y(A_{l,Y}), \mu_Y(A_{r,Y})$) into (10). Repeating this for each $t \in \mathcal{C}$ only requires locating the split index in the sorted arrays and reading prefix sums (or, if scanning thresholds in increasing order, just incrementing the split index), which is exactly why continuous splits can be evaluated efficiently once the values are sorted.

B.2. Efficient subset splitting for categorical covariates

We now show how to efficiently find the best split for a categorical coordinate. The approach is similar to that used in standard decision trees, as shown by Fisher (1958).

Problem setting (one categorical X -coordinate at one leaf). Fix a current leaf $A = A_X \times A_Y$ and a categorical covariate coordinate $z_\ell \in \Sigma = \{1, \dots, K\}$. We consider subset splits $S \subset \Sigma, S \neq \emptyset, \Sigma$:

$$A_l := A \cap \{z_\ell \in S\}, \quad A_r := A \cap \{z_\ell \notin S\}.$$

Since this is an X -split, both children share the same outcome side: $A_{l,Y} = A_{r,Y} = A_Y$, hence $\mu_Y(A_{l,Y}) = \mu_Y(A_{r,Y}) = \mu_Y(A_Y)$ is constant and cancels from the empirical gain (10).

For each category $c \in \Sigma$, define the per-category counts inside A :

$$a_c := n_{XY}(A \cap \{z_\ell = c\}), \quad b_c := n_X(A \cap \{z_\ell = c\}), \quad r_c := \frac{a_c}{b_c},$$

where we only consider categories with $b_c > 0$. For $S \subset \Sigma$ set

$$a_S := \sum_{c \in S} a_c, \quad b_S := \sum_{c \in S} b_c, \quad r_S := \frac{a_S}{b_S},$$

and similarly for S^c .

For an X -split, $\mu_Y(A_{l,Y}) = \mu_Y(A_{r,Y}) = \mu_Y(A_Y)$ is constant, and the parent term in (10) is constant in S . Dropping constants yields

$$G(S) \equiv a_S \log\left(\frac{a_S}{b_S}\right) + a_{S^c} \log\left(\frac{a_{S^c}}{b_{S^c}}\right) = b_S \varphi(r_S) + b_{S^c} \varphi(r_{S^c}). \quad (15)$$

which we seek to maximize.

Proposition B.1 (Optimal subset split is a sorted prefix). *Let $\varphi(u) := u \log u$ and let $D(u, v)$ be its Bregman divergence*

$$D(u, v) := \varphi(u) - \varphi(v) - \varphi'(v)(u - v) = u \log \frac{u}{v} - u + v.$$

Consequently, there exists a maximizer S^ of $G(S)$ such that, after sorting categories by r_c ,*

$$r_{\sigma(1)} \leq \dots \leq r_{\sigma(K)}, \quad S^* = \{\sigma(1), \dots, \sigma(t)\} \text{ for some } t \in \{1, \dots, K-1\}.$$

In particular, the best subset split can be found by sorting $\{r_c\}$ once and scanning the $K-1$ prefix thresholds using prefix sums of $\{a_c, b_c\}$.

Proof. Using $\sum_{c \in S} b_c(r_c - r_S) = 0$ and the definition of D , we have

$$\sum_{c \in S} b_c D(r_c, r_S) = \sum_{c \in S} b_c \varphi(r_c) - b_S \varphi(r_S),$$

and similarly for S^c . By rearranging and plugging into (15), we can see that the empirical gain of the categorical X -split S equals (up to additive constants independent of S):

$$G(S) \equiv b_S \varphi(r_S) + b_{S^c} \varphi(r_{S^c}) = \sum_{c \in \Sigma} b_c \varphi(r_c) - \left(\sum_{c \in S} b_c D(r_c, r_S) + \sum_{c \in S^c} b_c D(r_c, r_{S^c}) \right).$$

Let $u := r_S$ and $v := r_{S^c}$ and relabel children so that $u \leq v$. Consider the difference in divergence to the two centers for a point x :

$$\Delta(x) := D(x, u) - D(x, v).$$

A direct expansion shows $\Delta(x) = \alpha + \beta x$ with $\beta = \varphi'(v) - \varphi'(u) \geq 0$ (since φ' is increasing and $u \leq v$), so $\Delta(x)$ is non-decreasing in x . Hence, there exists a threshold t such that categories with $r_c \leq t$ weakly prefer u and those with $r_c > t$ weakly prefer v . Therefore, for fixed (u, v) , the assignment minimizing:

$$\sum_c b_c \min\{D(r_c, u), D(r_c, v)\}$$

is contiguous after sorting by r_c , i.e., a prefix split. Finally, for Bregman divergences, the minimizer over the center of $\sum_{c \in S} b_c D(r_c, \cdot)$ is the weighted mean r_S ; thus, re-centering after applying the threshold assignment cannot increase the cost. This yields an optimal split of prefix form. \square

Remark (categorical Y -splits). If the split acts on a categorical outcome coordinate $z_\ell \in \Sigma$ (a Y -split), then $n_X(\cdot)$ is constant across children ($n_X(A_l) = n_X(A_r) = n_X(A)$), but the μ_Y terms vary across subsets. In this case, the same sorted-prefix conclusion holds after redefining, for each category $c \in \Sigma$,

$$a_c := n_{XY}(A \cap \{z_\ell = c\}), \quad b_c := \mu_Y(A_Y \cap \{z_\ell = c\}), \quad r_c := \frac{a_c}{b_c},$$

and repeating the Bregman-threshold argument with these (a_c, b_c, r_c) .

Time complexity consequences. The prefix optimality avoids enumerating all $2^{|\Sigma|} - 2$ nontrivial subset splits. Instead, one computes per-category statistics (a_c, b_c) inside the leaf and sorts categories by $r_c = a_c/b_c$, then scans the $|\Sigma| - 1$ prefixes using prefix sums. This costs $O(n_{XY}(A) + |\Sigma| \log |\Sigma|)$ time (or $O(|\Sigma| \log |\Sigma|)$ once the per-category counts are available).

C. Consistency

We rephrase it here for clarity.

Corollary C.1. ([Lugosi & Nobel, 1996](#)) Let Z_1, Z_2, \dots be i.i.d. random vectors in $\mathcal{X} \times \mathcal{Y}$ with $Z_i \sim \lambda$, and let $\mathcal{A}_1, \mathcal{A}_2, \dots$ be a sequence of partition families. If N tends to infinity:

1. $N^{-1}m(\mathcal{A}_N) \rightarrow 0$
2. $N^{-1} \log \Delta_N^*(\mathcal{A}_N) \rightarrow 0$

Then

$$\sup_{\pi \in \mathcal{A}_N} \sum_{A \in \pi} |\lambda_N(A) - \lambda(A)| \rightarrow 0 \quad (16)$$

with probability one.

We now adapt the problem setting of ([Lugosi & Nobel, 1996](#)) to our setting. A N -sample partitioning rule π_N for \mathcal{Z} is a function that associates every N -set \mathcal{D}_N of \mathcal{Z}^N with a measurable partition $\pi(\mathcal{D}_N)$ of \mathcal{Z} . Let $\Pi = \{\pi_1, \pi_2, \dots\}$ be a partition scheme, defined as a sequence of partitioning rules. Every partitioning rule π_N is associated to a fixed non-random family of partitions $\mathcal{A} = \{\pi_N(\mathcal{D}_N) : \mathcal{D}_N \in \mathcal{Z}\}$, and every partitioning scheme is associated with a sequence $\{\mathcal{A}_1, \mathcal{A}_2, \dots\}$.

C.1. Truncation of \mathcal{Z}

The following lemma is used to ensure consistency between the tree algorithm and the truncation of \mathcal{Y} .

Lemma C.2 (Mass capture of the empirical min–max box). *Let $(\Omega, \mathcal{A}, \mathbb{P})$ be a probability triple. Let $\omega \in \Omega$, $Y \in \mathcal{Y}$, with $\mathcal{Y} := \mathbb{R}^{d_{y,c}}$ have distribution \mathbb{P}_Y and let Y_1, Y_2, \dots be i.i.d. copies of Y . Fix any deterministic padding sequence $\delta_N \geq 0$. Define for each coordinate j :*

$$\underline{y}_{N,j} := \min_{1 \leq i \leq N} (Y_i)_j, \quad \bar{y}_{N,j} := \max_{1 \leq i \leq N} (Y_i)_j,$$

and the random axis-aligned box

$$\bar{\mathcal{Y}}_N := \prod_{j=1}^{d_{y,c}} [\underline{y}_{N,j} - \delta_N, \bar{y}_{N,j} + \delta_N].$$

Then

$$\mathbb{P}_Y(\bar{\mathcal{Y}}_N^c) \xrightarrow{N \rightarrow \infty} 0 \quad \text{almost surely.}$$

Proof. Take $\epsilon \in (0, 1)$ and set $\alpha = \frac{\epsilon}{2d_y}$. For each coordinate $j \in \{1, \dots, d_{y,c}\}$ define the marginal Cumulative Distribution Function (CDF):

$$F_j(t) := \mathbb{P}(Y_j \leq t)$$

And the α and $1 - \alpha$ quantiles:

$$q_j^- = \inf\{t : F_j(t) \geq \alpha\}, \quad q_j^+ = \inf\{t : F_j(t) \geq 1 - \alpha\}$$

Consider the minimum and maximum observed values:

$$y_{N,j}^- = \min_{1 \leq i \leq N} (Y_i)_j, \quad y_{N,j}^+ = \max_{1 \leq i \leq N} (Y_i)_j$$

Consider the bad events:

$$E_{N,j}^- := \{y_{N,j}^- > q_j^-\}, \quad E_{N,j}^+ := \{y_{N,j}^+ < q_j^+\}$$

From independence of samples, $\mathbb{P}(E_{N,j}^-) = \mathbb{P}(y_{N,j}^- > q_j^-) = \mathbb{P}(Y_j > q_j^-)^N = (1 - F_j(q_j^-))^N \leq (1 - \alpha)^N$ and $\mathbb{P}(E_{N,j}^+) = \mathbb{P}(y_{N,j}^+ < q_j^+) = (\mathbb{P}(Y_j < q_j^+))^N = (\lim_{t \uparrow q_j^+} F_j(t))^N \leq (1 - \alpha)^N$. By Borel-Cantelli, since $\sum_{N \geq 1} \mathbb{P}(E_{N,j}^-) < \infty$

and $\sum_{N \geq 1} \mathbb{P}(E_{N,j}^+) < \infty$:

$$\mathbb{P}(E_{N,j}^- \text{ i.o.}) = 0, \quad \mathbb{P}(E_{N,j}^+ \text{ i.o.}) = 0$$

Therefore, for any given j , there exists $N_{0,j}(\omega)$ such that $y_{N,j}^- \leq q_j^-$ and $y_{N,j}^+ \geq q_j^+$ for all $N \geq N_{0,j}(\omega)$ almost surely. Take $N_0(\omega) = \max_j N_{0,j}(\omega)$. For all $N \geq N_0(\omega)$:

$$\prod_{j=1}^{d_{y,c}} [q_j^-, q_j^+] \subseteq \bar{\mathcal{Y}}_N$$

And:

$$\mathbb{P}(\bar{\mathcal{Y}}_N^c) = \mathbb{P}_Y\left(\left(\prod_{j=1}^{d_{y,c}} [y_{N,j}^- - \delta_N, y_{N,j}^+ + \delta_N]\right)^c\right) \leq \mathbb{P}_Y\left(\left(\prod_{j=1}^{d_{y,c}} [q_j^-, q_j^+]\right)^c\right)$$

Since

$$\left(\prod_{j=1}^{d_{y,c}} [q_j^-, q_j^+]\right)^c \subseteq \bigcup_{j=1}^{d_{y,c}} (\{Y_j < q_j^-\} \cup \{Y_j > q_j^+\})$$

we use the union bound:

$$\mathbb{P}(\bar{\mathcal{Y}}_N(\omega)^c) \leq \mathbb{P}_Y\left(\prod_{j=1}^{d_{y,c}} [q_j^-, q_j^+]^c\right) \leq \sum_{j=1}^{d_{y,c}} (\mathbb{P}_Y(Y_j < q_j^-) + \mathbb{P}_Y(Y_j > q_j^+)) \leq \sum_{j=1}^{d_{y,c}} 2\alpha = \epsilon$$

Since ϵ is arbitrary, we conclude $\mathbb{P}_Y(\bar{\mathcal{Y}}_N^c) \rightarrow 0$ almost surely. \square

Lemma C.2 applies to continuous \mathcal{Y} . For categorical coordinates, we do not truncate and do not need to worry about them. Therefore, if \mathcal{Y} is composed of a product of continuous and categorical dimensions, the Lemma also applies. The following proposition suggests that it is enough to study the consistency on $\bar{\mathcal{Z}}_N$ if such a random axis-aligned box is used:

C.2. Uniform bound for VC Dimension of X Partitions

In the main proof regarding consistency of data-driven partitions of \mathcal{Z} , the bound proven in the Lemma C.3 will be used.

Lemma C.3 (Almost-sure uniform VC deviation for $\hat{\mathbb{P}}_X$). *Let \mathcal{C}_X have VC dimension $V_X < \infty$. Then with probability one, for all sufficiently large N ,*

$$\sup_{U \in \mathcal{C}_X} |\hat{\mathbb{P}}_X(U) - \mathbb{P}_X(U)| \leq \sqrt{\frac{8}{N} \left(V_X \log(2eN/V_X) + \log(4N^2) \right)} = O\left(\sqrt{\frac{\log N}{N}}\right).$$

Proof. Let $\mathcal{F} := \{\mathbf{1}_U : U \in \mathcal{C}_X\}$. For $f \in \mathcal{F}$, write $\mathbb{P}f := \mathbb{E}[f(X)]$ and $\hat{\mathbb{P}}f := \frac{1}{N} \sum_{i=1}^N f(X_i)$.

Step 1: Symmetrization. Let X'_1, \dots, X'_N be an independent ghost sample with law \mathbb{P}_X , and let $\widehat{\mathbb{P}}' f := \frac{1}{N} \sum_{i=1}^N f(X'_i)$. For every $\varepsilon > 0$,

$$\mathbb{P}\left(\sup_{f \in \mathcal{F}} |\widehat{\mathbb{P}}f - \mathbb{P}f| > \varepsilon\right) \leq 2 \mathbb{P}\left(\sup_{f \in \mathcal{F}} |\widehat{\mathbb{P}}f - \widehat{\mathbb{P}}' f| > \varepsilon/2\right). \quad (17)$$

Step 2: Finite reduction and Hoeffding. Condition on the realized $2N$ points $(X_1, \dots, X_N, X'_1, \dots, X'_N)$. The supremum over $f \in \mathcal{F}$ depends only on the induced labeling of these $2N$ points, hence is a maximum over at most $\Delta_{\mathcal{C}_X}(2N)$ labelings. For a fixed labeling (equivalently, fixed f), the difference $\widehat{\mathbb{P}}f - \widehat{\mathbb{P}}' f$ is an average of N independent mean-zero terms in $[-1, 1]$, so Hoeffding gives

$$\mathbb{P}\left(|\widehat{\mathbb{P}}f - \widehat{\mathbb{P}}' f| > \varepsilon/2\right) \leq 2 \exp\left(-\frac{N\varepsilon^2}{8}\right).$$

A union bound over at most $\Delta_{\mathcal{C}_X}(2N)$ labelings and then (17) yield

$$\mathbb{P}\left(\sup_{U \in \mathcal{C}_X} |\widehat{\mathbb{P}}_X(U) - \mathbb{P}_X(U)| > \varepsilon\right) \leq 4 \Delta_{\mathcal{C}_X}(2N) \exp\left(-\frac{N\varepsilon^2}{8}\right). \quad (18)$$

Step 3: Sauer–Shelah. Since $\text{VCdim}(\mathcal{C}_X) = V_X$, Sauer–Shelah implies for $N \geq V_X$,

$$\Delta_{\mathcal{C}_X}(2N) \leq \left(\frac{2eN}{V_X}\right)^{V_X}.$$

Substituting into (18) gives, for $N \geq V_X$,

$$\mathbb{P}\left(\sup_{U \in \mathcal{C}_X} |\widehat{\mathbb{P}}_X(U) - \mathbb{P}_X(U)| > \varepsilon\right) \leq 4 \left(\frac{2eN}{V_X}\right)^{V_X} \exp\left(-\frac{N\varepsilon^2}{8}\right). \quad (19)$$

Part (1): High-probability bound. Choose $\varepsilon = \varepsilon_N(\delta)$ so that the right-hand side of (19) is at most δ :

$$\varepsilon_N(\delta) := \sqrt{\frac{8}{N} \left(V_X \log(2eN/V_X) + \log(4/\delta) \right)}.$$

Then

$$\mathbb{P}\left(\sup_{U \in \mathcal{C}_X} |\widehat{\mathbb{P}}_X(U) - \mathbb{P}_X(U)| > \varepsilon_N(\delta)\right) \leq \delta,$$

Part (2): Almost-sure bound (Borel–Cantelli). Set $\delta_N := N^{-2}$ and apply (1) with $\delta = \delta_N$:

$$\mathbb{P}\left(\sup_{U \in \mathcal{C}_X} |\widehat{\mathbb{P}}_X(U) - \mathbb{P}_X(U)| > \varepsilon_N(\delta_N)\right) \leq \delta_N.$$

Since $\sum_{N \geq 1} \delta_N < \infty$, Borel–Cantelli implies that with probability one, only finitely many of these events occur; equivalently, almost surely for all large N ,

$$\sup_{U \in \mathcal{C}_X} |\widehat{\mathbb{P}}_X(U) - \mathbb{P}_X(U)| \leq \varepsilon_N(\delta_N).$$

Finally,

$$\varepsilon_N(\delta_N) = \sqrt{\frac{8}{N} \left(V_X \log(2eN/V_X) + \log(4N^2) \right)} =: \varepsilon_N^{\text{a.s.}} = O\left(\sqrt{\log N/N}\right)$$

for all sufficiently large N . \square

C.3. Proof of Theorem 3.1

We now state the proof of the consistency theorem of data-driven partitions. For mixed spaces, we use a product metric that treats categorical coordinates with Hamming distance:

$$d_{\text{Ham}}(u, v) := \mathbf{1}\{u \neq v\}.$$

Define for $z = (x, y)$ and $z' = (x', y')$:

$$\begin{aligned} d_{\mathcal{Z}}(z, z') &:= \phi(\|(x^{(c)}, y^{(c)}) - (x'^{(c)}, y'^{(c)})\|_2) \\ &+ \sum_{j=1}^{d_{x,k}} d_{\text{Ham}}(x_j^{(k)}, x'^{(k)}_j) \\ &+ \sum_{j=1}^{d_{y,k}} d_{\text{Ham}}(y_j^{(k)}, y'^{(k)}_j). \end{aligned}$$

Then $\text{dist}_{d_{\mathcal{Z}}}(z, S) := \inf_{u \in S} d_{\mathcal{Z}}(z, u)$ for $S \subset \mathcal{Z}$.

Theorem 3.1. *Let $\mathcal{D}_N = \{(X_i, Y_i)\}_{i=1}^N = \{\mathcal{Z}_i\}_{i=1}^N$ be a set of observations belonging to $\mathcal{Z} := \mathcal{X} \times \mathcal{Y}$ with joint distribution $\mathbb{P}_{XY} \ll \nu$. Consider $\bar{\mathcal{Y}}_N$ a ν -measurable truncation of \mathcal{Y} as in Equation (6). Let $\Pi = \{\pi_1, \dots, \pi_N\}$ be a partitioning scheme for $\bar{\mathcal{Z}}_N := \mathcal{X} \times \bar{\mathcal{Y}}_N$, and let \mathcal{A}_N be the collection of partitions associated with the rule π_N . Denote by $f(X, Y)$ the conditional density of Y given X and the estimate as in Equation (7). Assume:*

1. $N^{-1}m(\mathcal{A}_N) \xrightarrow{N \rightarrow \infty} 0$
2. $N^{-1} \log \Delta_N^*(\mathcal{A}_N) \xrightarrow{N \rightarrow \infty} 0$
3. *There exists a sequence $\gamma_N \xrightarrow{N \rightarrow \infty} 0$ such that $\mathbb{P}_{XY}(\{z \in \bar{\mathcal{Z}}_N : \text{diam}(\pi_N[z]) > \gamma_N\}) \xrightarrow{N \rightarrow \infty} 0$*
4. $m_X(\mathcal{A}_N) \sqrt{\frac{\log N}{N}} \rightarrow 0$.

Then

$$\|\hat{f}_{\pi_N} - f\|_{L^1(\nu)} \rightarrow 0 \quad \text{as } N \rightarrow \infty,$$

almost surely.

Proof of Theorem 3.1. Let $\bar{\mathcal{Y}}_N$ be defined as in (6) and set $\bar{\mathcal{Z}}_N := \mathcal{X} \times \bar{\mathcal{Y}}_N$. We can write:

$$\|f_N - f\|_{L^1(\nu)} = \int_{\mathcal{X}} \int_{\bar{\mathcal{Y}}_N} |f_N - f| d\mu_Y d\mathbb{P}_X + \int_{\mathcal{X}} \int_{\bar{\mathcal{Y}}_N^c} |f_N - f| d\mu_Y d\mathbb{P}_X.$$

Since $f_N = 0$ on $\bar{\mathcal{Z}}_N^C$, the last term equals $\mathbb{P}_Y(\bar{\mathcal{Y}}_N^C)$, which goes to zero almost surely as $N \rightarrow \infty$ according to Lemma C.2. Therefore, we can focus on $\|f_N - f\|_{L^1(\nu; \bar{\mathcal{Z}}_N)}$.

Let:

$$f'_N(z) = \frac{\hat{\mathbb{P}}_{XY}(\pi_N[z])}{\mathbb{P}_X(\pi_N[z])\mu_Y(\pi_N[z])}, \quad f_N^* = \frac{\mathbb{P}_{XY}(\pi_N[z])}{\mathbb{P}_X(\pi_N[z])\mu_Y(\pi_N[z])}$$

By triangle inequality:

$$\|f_N - f\|_{L^1(\nu; \bar{\mathcal{Z}}_N)} \leq \underbrace{\|f_N - f'_N\|_{L^1(\nu; \bar{\mathcal{Z}}_N)}}_{(I)} + \underbrace{\|f'_N - f_N^*\|_{L^1(\nu; \bar{\mathcal{Z}}_N)}}_{(II)} + \underbrace{\|f_N^* - f\|_{L^1(\nu; \bar{\mathcal{Z}}_N)}}_{(III)}.$$

Bounding (I)

$$\begin{aligned}
 \|f_N - f'_N\|_{L^1(\nu; \bar{\mathcal{Z}}_N)} &= \left\| \frac{\hat{\mathbb{P}}_{XY}}{\hat{\mathbb{P}}_X \mu_Y} - \frac{\hat{\mathbb{P}}_{XY}}{\mathbb{P}_X \mu_Y} \right\|_{L^1(\nu; \bar{\mathcal{Z}}_N)} = \left\| \frac{\hat{\mathbb{P}}_{XY}}{\hat{\mathbb{P}}_X \mu_Y} \left(\frac{\mathbb{P}_X - \hat{\mathbb{P}}_X}{\hat{\mathbb{P}}_X} \right) \right\|_{L^1(\nu; \bar{\mathcal{Z}}_N)} \\
 &= \sum_{A \in \pi_N} \left| \frac{\hat{\mathbb{P}}_{XY}(A)}{\mathbb{P}_X(A) \mu_Y(A)} \left(\frac{\mathbb{P}_X(A) - \hat{\mathbb{P}}_X(A)}{\hat{\mathbb{P}}_X(A)} \right) \right| \mathbb{P}_X(A) \mu_Y(A) \\
 &= \sum_{A \in \pi_N} \left| \frac{\hat{\mathbb{P}}_{XY}(A)}{\hat{\mathbb{P}}_X(A)} (\mathbb{P}_X(A) - \hat{\mathbb{P}}_X(A)) \right|
 \end{aligned}$$

The key point is that the A_X 's may overlap, so we *cannot* invoke a partition-based bound on the sum. Instead, we group terms by *distinct* projected sets. Let \mathcal{C}_X denote the collection of all covariate regions in \mathcal{X} that can arise as the X -projection of a leaf by iterating the permitted split tests (axis-aligned threshold splits for continuous features and subset-membership splits for categorical features). Assume that \mathcal{C}_X has finite VC dimension, and denote $V_X := \text{VCdim}(\mathcal{C}_X)$.

Let

$$\mathcal{U}(\pi_N) := \{A_X : A \in \pi_N\} \subseteq \mathcal{C}_X,$$

and for each $U \in \mathcal{U}(\pi_N)$ define

$$w_U := \sum_{A \in \pi_N : A_X = U} \frac{\hat{\mathbb{P}}_{XY}(A)}{\hat{\mathbb{P}}_X(U)}.$$

Because $\bigcup_{A: A_X = U} A \subseteq U \times \mathcal{Y}$ and empirical mass is additive over disjoint leaves,

$$\sum_{A: A_X = U} \hat{\mathbb{P}}_{XY}(A) \leq \hat{\mathbb{P}}_{XY}(U \times \bar{\mathcal{Y}}_N) = \hat{\mathbb{P}}_X(U),$$

hence $0 \leq w_U \leq 1$. Therefore

$$\begin{aligned}
 \|f_N - f'_N\|_{L^1(\nu; \bar{\mathcal{Z}}_N)} &= \sum_{U \in \mathcal{U}(\pi_N)} w_U |\mathbb{P}_X(U) - \hat{\mathbb{P}}_X(U)| \leq \sum_{U \in \mathcal{U}(\pi_N)} |\mathbb{P}_X(U) - \hat{\mathbb{P}}_X(U)| \\
 &\leq |\mathcal{U}(\pi_N)| \cdot \sup_{U \in \mathcal{C}_X} |\mathbb{P}_X(U) - \hat{\mathbb{P}}_X(U)|.
 \end{aligned}$$

Now apply Lemma C.3: $\sup_{U \in \mathcal{C}_X} |\mathbb{P}_X(U) - \hat{\mathbb{P}}_X(U)|$ is almost surely bounded with rate $O(\sqrt{\log N/N})$. Also, $\mathcal{U}(\pi_N) \leq m_X(\mathcal{A}_N)$. Consequently, if

$$m_X(\mathcal{A}_N) \sqrt{\frac{\log N}{N}} \rightarrow 0,$$

then by condition 4. (I) = $\|f_N - f'_N\|_{L^1(\nu; \bar{\mathcal{Z}}_N)} \rightarrow 0$ almost surely.

Bounding (II)

$$\|f'_N - f_N^*\|_{L^1(\nu; \bar{\mathcal{Z}}_N)} = \left\| \frac{1}{\hat{\mathbb{P}}_X \mu_Y} (\hat{\mathbb{P}}_{XY} - \mathbb{P}_{XY}) \right\|_{L^1(\nu; \bar{\mathcal{Z}}_N)} = \sum_{A \in \pi_N} |\hat{\mathbb{P}}_{XY}(A) - \mathbb{P}_{XY}(A)|$$

Applying Corollary C.1 and conditions 1 and 2, this term also converges to 0.

Bounding (III) To bound the term (III), we use a similar strategy to (Lugosi & Nobel, 1996), but in a more general setting where $\mathcal{X} \times \mathcal{Y}$ can be composed of integer-valued, discrete, or categorical dimensions.

Since $(\mathcal{Z}, d_{\mathcal{Z}})$ is a separable metric space and ν is a Borel measure, for every $\varepsilon > 0$ there exists a nonnegative simple function $g = \sum_{j=1}^J a_j \mathbf{1}_{G_j}$ with pairwise disjoint $G_j \subseteq \mathcal{Z}$ and $\nu(\partial G_j) = 0$ such that

$$\|f - g\|_{L^1(\nu)} < \varepsilon.$$

In particular,

$$\|f - g\|_{L^1(\nu; \bar{\mathcal{Z}}_N)} \leq \|f - g\|_{L^1(\nu)} < \varepsilon.$$

Define

$$g_N(z) := \frac{\int_{\pi_N[z]} g d\nu}{\nu(\pi_N[z])}.$$

We split (III) into three components, based on these newly introduced functions g and g_N :

$$\|f_N^* - f\|_{L^1(\nu; \bar{\mathcal{Z}}_N)} \leq \underbrace{\|f_N^* - g_N\|_{L^1(\nu; \bar{\mathcal{Z}}_N)}}_{(*)} + \underbrace{\|g_N - g\|_{L^1(\nu; \bar{\mathcal{Z}}_N)}}_{(\dagger)} + \underbrace{\|g - f\|_{L^1(\nu; \bar{\mathcal{Z}}_N)}}_{< \varepsilon}$$

The third term is bounded by definition. Bounding (*):

$$\|f_N^* - g_N\|_{L^1(\nu; \bar{\mathcal{Z}}_N)} = \int_{\bar{\mathcal{Z}}_N} |f_N^* - g_N| d\nu = \sum_{A \in \pi_N} \left| \int_A f d\nu - \int_A g d\nu \right| \quad (20)$$

$$\leq \sum_{A \in \pi_N} \int_A |f - g| d\nu = \int_{\bar{\mathcal{Z}}_N} |f - g| d\nu < \varepsilon \quad (21)$$

To bound (\dagger) , let $M := \|g\|_\infty = \max_{j \in \{1, \dots, J\}} a_j$. Let ∂G_j denote the topological boundary of G_j , $\nu(\partial G_j) = 0$ for all $j \in \{1, \dots, J\}$. Choose $1 > \eta > 0$ and define two sets:

$$U(\eta) := \bigcup_{j=1}^J \{z \in \bar{\mathcal{Z}}_N : \text{dist}_{d_{\mathcal{Z}}}(z, \partial G_j) \leq \eta\}$$

$$D_N(\eta) = D_N^{\text{cont}}(\eta) \cup D_N^{\text{cat}}$$

where $D_N^{\text{cont}}(\eta) = \{z \in \bar{\mathcal{Z}}_N : \text{diam}_{\text{cont}}(\pi_N[z]) > \eta\}$ and $D_N^{\text{cat}} = \{z : \exists k \text{ s.t. } |S_k(\pi_N[z])| > 1\}$.

We study (\dagger) in two disjoint domains: $\bar{\mathcal{Z}}_N \setminus (U(\eta) \cup D_N(\eta))$ and $U(\eta) \cup D_N(\eta)$.

Claim 1. For all, $z \in \bar{\mathcal{Z}}_N \setminus (U(\eta) \cup D_N(\eta))$ we have $g_N = g$ and $\int_{\bar{\mathcal{Z}}_N \setminus (U(\eta) \cup D_N(\eta))} |g_N - g| d\nu = 0$.

Proof. Pick $z \in \bar{\mathcal{Z}}_N \setminus U(\eta)$. Then there exists a G_j such that $z \in G_j$ and $\text{dist}_{d_{\mathcal{Z}}}(z, \partial G_j) > \eta$. Let $B(z, \eta) \subseteq G_j$ denote a ball of radius η centered on z . If, in addition, $z \notin D_N(\eta)$ then (i) $|S_k(\pi_N[z])| = 1$ for every categorical coordinate k , so $d_{\mathcal{Z}}(z, u) = d_{\text{cont}}(z, u)$ for all $u \in \pi_N[z]$, and (ii) $\text{diam}_{\text{cont}}(\pi_N[z]) \leq \eta$, hence $d_{\text{cont}}(z, u) \leq \eta$ for all $u \in \pi_N[z]$.

Therefore $d_{\mathcal{Z}}(z, u) \leq \eta$ for all $u \in \pi_N[z]$, i.e. $\pi_N[z] \subseteq B(z, \eta)$. Hence $\pi_N[z] \subseteq B(z, \eta) \subseteq G_j$. This implies $g = a_j$ on $\pi_N[z]$ and $g_N = g$. \square

Now we focus on $z \in U(\eta) \cup D_N(\eta)$. With the claim above, we have:

$$\|g_N - g\|_{L^1(\nu; \bar{\mathcal{Z}}_N)} \leq \int_{U(\eta) \cup D_N(\eta)} |g_N - g| d\nu \leq \int_{D_N(\eta)} |g_N - g| d\nu + \int_{U(\eta)} |g_N - g| d\nu \quad (22)$$

Since ∂G_j is closed and $\nu(\partial G_j) = 0$, we have

$$\{z : \text{dist}_{d_{\mathcal{Z}}}(z, \partial G_j) \leq \eta\} \downarrow \partial G_j \quad (\eta \downarrow 0),$$

hence by continuity from above for finite measures, $\nu(\{z : \text{dist}_{d_Z}(z, \partial G_j) \leq \eta\}) \rightarrow \nu(\partial G_j) = 0$. Therefore $\nu(U(\eta)) \rightarrow 0$ as $\eta \downarrow 0$. Since $|g| \leq M$ and $|g_N| \leq M$, the second term of (22) goes to zero as $\eta \rightarrow 0$:

$$\int_{U(\eta)} |g_N - g| d\nu \leq 2M \int_{U(\eta)} d\nu = 2M\nu(U(\eta)) \xrightarrow{\eta \rightarrow 0} 0$$

Let $\pi_N^\eta := \{A \in \pi_N : \text{diam}_{\text{cont}}(A) > \eta \text{ or } \exists k \text{ s.t. } |S_k(A)| > 1\}$. With respect to the first term of (22):

$$\int_{D_N(\eta)} |g_N - g| d\nu \leq 2 \int_{D_N(\eta)} |g_N| + |g| d\nu = 2 \int_{D_N(\eta)} |g| d\nu \quad (23)$$

$$= 2 \int_{D_N(\eta)} |g - f + f| d\nu \quad (24)$$

$$\leq 2\mathbb{P}_{XY}(D_N(\eta)) + 2 \int_{D_N(\eta)} |g - f| d\nu \quad (25)$$

$$< 2\mathbb{P}_{XY}(D_N(\eta)) + 2\varepsilon \quad (26)$$

We now show how condition 3 implies that the first term goes to zero as N tends to infinity. Fix any $\eta > 0$. Let $c_{\min} = \min_k \frac{1}{|\Sigma_k| - 1}$ denote the minimum length of a cell of π_N along a categorical dimension. Let $\gamma_N < \min(\eta, c_{\min})$. Then:

1. If $z \in D_N^{\text{cont}}(\eta)$, then $\text{diam}(\pi_N[z]) \geq \text{diam}_{\text{cont}}(\pi_N[z]) > \eta > \gamma_N$
2. If $z \in D_N^{\text{cat}}$, then $\text{diam}(\pi_N[z]) \geq c_{\min} > \gamma_N$

For all large N :

$$D_N(\eta) \subseteq \{z \in \bar{\mathcal{Z}}_N : \text{diam}(\pi_N[z]) > \gamma_N\}$$

so $\mathbb{P}_{XY}(D_N(\eta)) < \mathbb{P}_{XY}(\{z : \text{diam}(\pi_N[z]) > \gamma_N\}) \xrightarrow{N \rightarrow \infty} 0$. This finishes the proof for (\dagger) .

Finally, we have, as $N \rightarrow \infty$:

$$\|f_N - f\|_{L^1(\nu; \bar{\mathcal{Z}}_N)} < 4\varepsilon \quad (27)$$

Since ε is arbitrary, this proves the convergence for \dagger and therefore the proof is concluded. \square

C.4. Hybrid Tree Algorithm Satisfies Conditions for Consistency

In this section, we show that the proposed algorithm satisfies the conditions for consistency.

Lemma C.4. *Consider a tree algorithm that partitions $\bar{\mathcal{Z}}_N$ with a maximum budget of k_N splits. If $k_N = o(\sqrt{\frac{N}{\log N}})$, $k_N \rightarrow \infty$, then conditions 1., 2. and 4. of Theorem 3.1 are met.*

Proof. To check condition 1, note that with k splits, there are $k + 1$ leaves and $m(\mathcal{A}_N) = \sup_{\pi \in \mathcal{A}_N} |\pi| = k + 1$. Then $N^{-1}m(\mathcal{A}_N) \rightarrow 0$ as $N \rightarrow \infty$ whenever $k_N = o(N)$, which is satisfied by $o(\sqrt{N/\log(N)})$.

Now, we verify condition 2. Each split partitions the current sample indices by one coordinate test. For a continuous coordinate, the number of distinct dichotomies on N points is at most N (threshold between two consecutive sorted values).

For a categorical coordinate with finite alphabet size q , the number of distinct subset splits is at most $2^q - 2$, which is a constant independent of N .

Let d_{thr} be the number of coordinates eligible for threshold splits, and let $C_{\text{cat}} := \sum_{j=1}^{d_{\text{cat}}} (2^{q_j} - 2)$ be the total number of categorical subset tests across categorical coordinates (finite alphabets). Then the number of distinct 2-way splits available at any node is at most

$$S_N \leq N^{d_{\text{thr}}} \cdot (1 + C_{\text{cat}}),$$

hence a crude upper bound for the growth function of k -split trees is

$$\Delta_N^*(\mathcal{A}_N) \leq (S_N)^{k+1}.$$

Therefore,

$$\frac{1}{N} \log \Delta_N^*(\mathcal{A}_N) \leq \frac{k+1}{N} \left(d_{\text{thr}} \log N + \log(1 + C_{\text{cat}}) \right),$$

The RHS goes to zero if $k = o(N/\log N)$, which is also satisfied by $k = o(\sqrt{N/\log N})$, and we have checked condition 2.

With respect to condition 4, under axis-aligned threshold splits on (\mathbb{R}^{d_c}) and subset-membership splits on categorical coordinates with finite alphabets, each leaf (X)-region is a product of an axis-aligned rectangle and a categorical cylinder set. Hence the induced class (\mathcal{C}_X) has finite VC dimension. Also, we have that $m_X(\mathcal{A}_N) \leq m(\mathcal{A}_N)$, then $k_N = o(\sqrt{\frac{N}{\log N}}) \implies m_X(\mathcal{A}_N) \sqrt{\frac{\log N}{N}} \rightarrow 0$. \square

Lemma C.4 showed that the tree algorithm can satisfy conditions 1,2, and 4. We now show that under some conditions, the tree algorithm also satisfies condition 3.

For condition 3, we need a splitting strategy that guarantees the shrinkage of cell sizes. The negative log-likelihood gain might not achieve this, since there might be distributions where one-step gain is zero, but there is a non-negligible oscillation of the conditional density.

Exploration contraction assumption. Throughout this appendix, whenever the hybrid tree construction is considered, we assume that every exploration split satisfies the uniform contraction property stated in Theorem 3.2, i.e.,

$$\max(\text{diam}(A_1), \text{diam}(A_r)) \leq \rho \text{diam}(A) \quad \text{for some } \rho \in [1/2, 1].$$

Lemma C.5 (Deterministic shrinkage under greedy splitting of the largest leaf). *Let π_N be constructed by starting from $\bar{\mathcal{Z}}_N$ and performing $k_{N,e}$ splits, with $k_{N,e} \rightarrow \infty$ as $N \rightarrow \infty$. Assume: (i) at each step, the algorithm splits a current leaf A with the largest diameter (ties arbitrary); and (ii) every split $A \rightarrow \{A_l, A_r\}$ satisfies*

$$\max(\text{diam}(A_l), \text{diam}(A_r)) \leq \rho \text{diam}(A) \quad \text{for some } \rho \in [0.5, 1].$$

Then, letting $n_s := \lfloor \log_2(k_{N,e} + 1) \rfloor$ and $\gamma_N = \text{diam}(\bar{\mathcal{Z}}_N) \rho^{n_s}$

$$\mathbb{P}_{XY}(\{z \in \bar{\mathcal{Z}}_N : \text{diam}(\pi_N[z]) > \gamma_N\}) = 0$$

Proof. Define $M_s := \max_{A \in \pi_N^{(s)}} \text{diam}(A)$ as the maximum leaf diameter after s splits, where $\pi_N^{(0)} = \{\bar{\mathcal{Z}}_N\}$ and $\pi_N^{(k_{N,e})} = \pi_N$.

We prove by induction on $m \geq 0$ that

$$M_{2^m-1} \leq \text{diam}(\bar{\mathcal{Z}}_N) \rho^m. \tag{28}$$

Base case $m = 0$. Here $2^0 - 1 = 0$ and $M_0 = \text{diam}(\bar{\mathcal{Z}}_N) = \text{diam}(\bar{\mathcal{Z}}_N) \rho^0$.

Inductive step. Assume (28) holds for some m . At time $2^m - 1$, there are exactly 2^m leaves, and each has diameter at most $M_{2^m-1} \leq \text{diam}(\bar{\mathcal{Z}}_N) \rho^m$. Now perform the next 2^m splits, i.e., go from $2^m - 1$ splits to $2^{m+1} - 1$ splits.

Each split is applied to a leaf of the current maximum diameter (by assumption), and each child has a diameter at most ρ times its parent. Since every parent split during this stage has a diameter at most $\text{diam}(\bar{\mathcal{Z}}_N)\rho^m$, every newly created leaf has diameter at most $\text{diam}(\bar{\mathcal{Z}}_N)\rho^{m+1}$.

It remains to show that after these 2^m greedy splits, there cannot remain any leaf with diameter exceeding $\text{diam}(\bar{\mathcal{Z}}_N)\rho^{m+1}$. Suppose, toward a contradiction, that some leaf B with $\text{diam}(B) > \text{diam}(\bar{\mathcal{Z}}_N)\rho^{m+1}$ remains unsplit throughout this stage. All new leaves created during this stage have a diameter of at most $\text{diam}(\bar{\mathcal{Z}}_N)\rho^{m+1}$, hence strictly smaller than $\text{diam}(B)$. Therefore, at each split time during this stage, B would be among the leaves of maximal diameter and must be selected by the greedy rule, contradicting that it was never split. Thus, at time $2^{m+1} - 1$, all leaves have diameter at most $\text{diam}(\bar{\mathcal{Z}}_N)\rho^{m+1}$, proving (28) for $m + 1$.

This completes the induction.

Now set $n_s = \lfloor \log_2(k_{N,e} + 1) \rfloor$. Then $2^{n_s} - 1 \leq k_{N,e}$, and since splitting cannot increase the maximum diameter under the contraction property,

$$\sup_{A \in \pi_N} \text{diam}(A) = M_{k_{N,e}} \leq M_{2^{n_s} - 1} \leq \text{diam}(\bar{\mathcal{Z}}_N)\rho^{n_s}.$$

Note that for the diameter definition $\text{diam}(\mathcal{Z}) < \infty$, and $\text{diam}(\bar{\mathcal{Z}}_N) \leq \text{diam}(\mathcal{Z})$. Therefore, setting $\gamma_N = \text{diam}(\bar{\mathcal{Z}}_N)\rho^{\lfloor \log_2(k_{N,e} + 1) \rfloor}$ we have the desired result. \square

Finally, we can use Theorem 3.1 and Lemmas C.5 and C.4 to prove the Theorem 3.2.

Theorem 3.2. *(Consistency of the hybrid tree conditional density estimator)* Let \hat{f}_{π_N} be the tree estimator in (7), built from a best-first greedy construction that (i) uses the empirical log-loss gain (10) for its main split selection, and (ii) additionally allocates an exploration budget $k_{N,e}$ that always splits the current largest leaf.

Assume:

1. The total split budget satisfies $k_N = o(\sqrt{\frac{N}{\log N}})$ and $k_N \rightarrow \infty$. (e.g. $\sqrt[a]{N}$, $a > 2$), and the exploration budget $k_{N,e}$ satisfies $0 \leq k_{N,e} \leq k_N$ and $k_{N,e} \rightarrow \infty$.
2. (Per-split contraction for exploration) Every exploration split $A \rightarrow \{A_l, A_r\}$ satisfies $\max(\text{diam}(A_l), \text{diam}(A_r)) \leq \rho \text{diam}(A)$ for some $\rho \in [1/2, 1]$.

Then

$$\|\hat{f}_{\pi_N} - f\|_{L^1(\nu)} \longrightarrow 0 \quad \text{as } N \rightarrow \infty,$$

almost surely.

Proof. The first assumption implies that conditions 1., 2., and 4. of Theorem 3.1 are met (Lemma C.4). The second assumption implies condition 3 by Lemma C.5. \square

C.5. Normalization preserves $L^1(\nu)$ -consistency

In practice, we may normalize a nonnegative estimator $h_N(x, \cdot)$ to integrate to one with respect to μ_Y . The following lemma shows that this operation does not affect $L^1(\nu)$ consistency, where $\nu = \mathbb{P}_X \otimes \mu_Y$.

Lemma C.6 (Normalization preserves $L^1(\nu)$ -consistency). *Let μ_Y be a σ -finite measure on \mathcal{Y} and let $\nu := \mathbb{P}_X \otimes \mu_Y$. Assume $\mathbb{P}_{XY} \ll \nu$ and let*

$$f := \frac{d\mathbb{P}_{XY}}{d(\mathbb{P}_X \otimes \mu_Y)}.$$

Let $h_N : \mathcal{X} \times \mathcal{Y} \rightarrow [0, \infty)$ be measurable and define

$$s_N(x) := \int_{\mathcal{Y}} h_N(x, y) \mu_Y(dy), \quad \bar{h}_N(x, y) := \begin{cases} h_N(x, y)/s_N(x), & s_N(x) > 0, \\ 0, & s_N(x) = 0. \end{cases}$$

If $\|h_N - f\|_{L^1(\nu)} \rightarrow 0$, then $\|\bar{h}_N - f\|_{L^1(\nu)} \rightarrow 0$. Moreover, for all N ,

$$\|\bar{h}_N - f\|_{L^1(\nu)} \leq 6 \|h_N - f\|_{L^1(\nu)}.$$

Proof. Define the pointwise $L^1(\mu_Y)$ error

$$\xi_N(x) := \int_{\mathcal{Y}} |h_N(x, y) - f(x, y)| \mu_Y(dy),$$

so that $\mathbb{E}_{\mathbb{P}_X}[\xi_N] = \|h_N - f\|_{L^1(\nu)}$ by Tonelli's theorem. Next define the “good” set

$$E_N := \{x \in \mathcal{X} : \xi_N(x) \leq 1/2\}.$$

Since $\int_{\mathcal{Y}} f(x, y) \mu_Y(dy) = 1$ for \mathbb{P}_X -a.e. x , we have for such x ,

$$|1 - s_N(x)| = \left| \int_{\mathcal{Y}} (f(x, y) - h_N(x, y)) \mu_Y(dy) \right| \leq \int_{\mathcal{Y}} |f(x, y) - h_N(x, y)| \mu_Y(dy) = \xi_N(x).$$

Hence, on E_N we have $s_N(x) \geq 1 - |\xi_N(x)| \geq 1 - \xi_N(x) \geq 1/2$, so \bar{h}_N is well-defined there.

We decompose the $L^1(\nu)$ error into contributions over E_N and its complement:

$$\|\bar{h}_N - f\|_{L^1(\nu)} = \int_{E_N} \int_{\mathcal{Y}} |\bar{h}_N - f| \mu_Y(dy) \mathbb{P}_X(dx) + \int_{E_N^c} \int_{\mathcal{Y}} |\bar{h}_N - f| \mu_Y(dy) \mathbb{P}_X(dx). \quad (29)$$

Step 1: bound on E_N . Fix $x \in E_N$. Using the triangle inequality,

$$\int_{\mathcal{Y}} |\bar{h}_N - f| \mu_Y(dy) \leq \int_{\mathcal{Y}} |\bar{h}_N - h_N| \mu_Y(dy) + \int_{\mathcal{Y}} |h_N - f| \mu_Y(dy) = \int_{\mathcal{Y}} |\bar{h}_N - h_N| \mu_Y(dy) + \xi_N(x).$$

Moreover, for $x \in E_N$ (so $s_N(x) > 0$),

$$\int_{\mathcal{Y}} |\bar{h}_N - h_N| \mu_Y(dy) = \int_{\mathcal{Y}} h_N(x, y) \left| \frac{1}{s_N(x)} - 1 \right| \mu_Y(dy) = \left| \frac{1}{s_N(x)} - 1 \right| \int_{\mathcal{Y}} h_N(x, y) \mu_Y(dy) = |1 - s_N(x)|.$$

Combining with $|1 - s_N(x)| \leq \xi_N(x)$ yields

$$\int_{\mathcal{Y}} |\bar{h}_N - f| \mu_Y(dy) \leq 2 \xi_N(x) \quad \text{for all } x \in E_N.$$

Integrating over E_N gives

$$\int_{E_N} \int_{\mathcal{Y}} |\bar{h}_N - f| \mu_Y(dy) \mathbb{P}_X(dx) \leq 2 \int_{E_N} \xi_N(x) \mathbb{P}_X(dx) \leq 2 \|h_N - f\|_{L^1(\nu)}. \quad (30)$$

Step 2: bound on E_N^c . For any x , both $f(x, \cdot)$ and $\bar{h}_N(x, \cdot)$ are nonnegative and satisfy

$$\int_{\mathcal{Y}} f(x, y) \mu_Y(dy) = 1 \quad \text{and} \quad \int_{\mathcal{Y}} \bar{h}_N(x, y) \mu_Y(dy) \leq 1,$$

where the second inequality follows from the definition of \bar{h}_N (it equals 1 when $s_N(x) > 0$ and equals 0 otherwise). Therefore, for all x ,

$$\int_{\mathcal{Y}} |\bar{h}_N - f| \mu_Y(dy) \leq \int_{\mathcal{Y}} \bar{h}_N \mu_Y(dy) + \int_{\mathcal{Y}} f \mu_Y(dy) \leq 2.$$

Hence

$$\int_{E_N^c} \int_{\mathcal{Y}} |\bar{h}_N - f| \mu_Y(dy) \mathbb{P}_X(dx) \leq 2 \mathbb{P}_X(E_N^c). \quad (31)$$

It remains to bound $\mathbb{P}_X(E_N^c)$. By Markov's inequality,

$$\mathbb{P}_X(E_N^c) = \mathbb{P}_X(\xi_N > 1/2) \leq 2 \mathbb{E}_{\mathbb{P}_X}[\xi_N] = 2 \|h_N - f\|_{L^1(\nu)}.$$

Substituting into (31) gives

$$\int_{E_N^c} \int_{\mathcal{Y}} |\bar{h}_N - f| \mu_Y(dy) \mathbb{P}_X(dx) \leq 4 \|h_N - f\|_{L^1(\nu)}. \quad (32)$$

Step 3: conclude. Combining (29), (30), and (32) yields

$$\|\bar{h}_N - f\|_{L^1(\nu)} \leq 6 \|h_N - f\|_{L^1(\nu)}.$$

In particular, if $\|h_N - f\|_{L^1(\nu)} \rightarrow 0$, then $\|\bar{h}_N - f\|_{L^1(\nu)} \rightarrow 0$. \square

Corollary C.7. Consider the setting in Theorem 3.1 and the definition of \bar{f}_{π_N} as in Equation (8). Then

$$\|\bar{f}_{\pi_N} - f\|_{L^1(\nu)} \rightarrow 0 \quad \text{as } N \rightarrow \infty,$$

almost surely.

Proof. Use Theorem 3.1 and Lemma C.6. \square

D. Experiments

In this appendix, we describe the datasets used in the experiments, the hyperparameter tuning search space, and provide results on classification accuracy and Root mean squared error (RMSE) for regression tasks.

D.1. Datasets

Tables 3 and 4 summarize the information for the datasets used in this experiment, ordered by sample size. We use datasets ranging from 150 (Iris) to 48842 (Adult) samples in classification. The dataset with the largest alphabet for the target variable is Letter Recognition.

In regression, datasets range from 442 (Diabetes) to 45730 samples. Naval Propulsion Plant is the dataset with the largest number of features.

Table 3. Classification datasets ordered by sample size.

Dataset	Size	d_x	Classes	Reference
Iris	150	4	3	Fisher (1936)
Breast Cancer	286	9	2	Zwitter & Soklic (1988)
Wine	1599	11	6	Cortez et al. (2009)
Digits	1797	64	10	Alpaydin & Kaynak (1998)
Spam Base	4601	57	2	Hopkins et al. (1999)
Support2	9105	42	2	Harrell Jr & Harrell Jr (2019)
Letter Recognition	20000	16	26	Frey & Slate (1991)
Bank Marketing	45211	16	2	Moro et al. (2014)
Adult	48842	14	4	Kohavi & Becker (1996)

Table 4. Regression datasets ordered by sample size.

Dataset	Sample size	Features	Reference
Diabetes	442	10	Kahn (1994)
Boston	506	13	Harrison Jr & Rubinfeld (1978)
Energy Efficiency	768	8	Tsanas & Xifara (2012)
Concrete Compressive Strength	1030	8	Yeh (1998)
Kin8Nm	8192	8	Corke (2002)
Air Quality	9357	12	De Vito et al. (2008)
Power Plant	9568	4	Tüfekci (2014)
Naval Propulsion Plant	11934	14	Coraddu et al. (2016)
California Housing	20640	8	Pace & Barry (1997)
Physicochemical Protein	45730	9	Rana (2013)

D.2. Hyperparameter Tuning

All methods were tuned using Optuna with 200 trials and a 20-minute timeout per model. Cross-validation employed an 80/20 train-test split within each fold. For classification, the scoring metric was negative log-loss, while for regression, log-loss from the skpro library was used to optimize probabilistic predictions.

D.2.1. CLASSIFICATION METHODS

Partition Tree was tuned over two regularization parameters: the minimum number of samples required at a leaf node ($\text{min_samples_leaf} \in [1, 100]$) and the minimum number of samples in the feature space at each leaf ($\text{min_samples_leaf_x} \in [1, 400]$).

Partition Forest, the ensemble extension of Partition Tree, included additional hyperparameters controlling the subsampling strategy: the fraction of features to consider at each split ($\text{max_features} \in [0.7, 1.0]$) and the fraction of samples to draw

for each tree ($\text{max_samples} \in [0.7, 1.0]$), along with the same leaf constraints as Partition Tree.

XGBoost was tuned over five hyperparameters: the number of boosting rounds ($\text{n_estimators} \in [1, 200]$), tree depth ($\text{max_depth} \in [1, 3]$), learning rate ($\text{learning_rate} \in [0.01, 0.3]$, log-scale), minimum loss reduction for splits ($\text{min_split_loss} \in [0.0, 5.0]$), and minimum child weight ($\text{min_child_weight} \in [1, 100]$).

Random Forest was tuned over tree depth ($\text{max_depth} \in [3, 50]$), minimum samples required to split ($\text{min_samples_split} \in [2, 150]$), and minimum samples at leaf nodes ($\text{min_samples_leaf} \in [1, 100]$).

Decision Tree used the same hyperparameter space as Random Forest, with an additional parameter for minimum impurity decrease ($\text{min_impurity_decrease} \in [0.0, 0.1]$).

NGBoost employed a decision tree regressor as its base learner, following the natural gradient boosting framework. The base learner's hyperparameters were tuned ($\text{max_depth} \in [1, 3]$, $\text{min_samples_split} \in [2, 150]$, $\text{min_samples_leaf} \in [1, 100]$), along with the ensemble parameters ($\text{n_estimators} \in [1, 200]$ and $\text{learning_rate} \in [0.01, 0.3]$, log-scale).

D.2.2. REGRESSION METHODS

For probabilistic regression, several methods were wrapped with the `ResidualDouble` framework from `skpro`, which fits a secondary model to predict residual variance, enabling uncertainty quantification from point estimators.

Partition Tree (regression) was tuned over four parameters: the minimum samples in the target space ($\text{min_samples_leaf_y} \in [1, 400]$), minimum samples in the feature space ($\text{min_samples_leaf_x} \in [1, 400]$), a boundary expansion factor ($\text{boundaries_expansion_factor} \in [0.001, 0.1]$) that controls density estimation at partition boundaries, and $\text{min_target_volume} \in [0.01, 0.2]$, that limits the minimum volume $\mu_Y(A_y)$ of a cell to be valid.

Partition Forest (regression) included the same parameters as Partition Tree, plus subsampling controls: $\text{max_features} \in [0.7, 1.0]$ and $\text{max_samples} \in [0.7, 1.0]$.

XGBoost with ResidualDouble (Gressmann & Kiraly, 2018) was tuned over the same hyperparameters as in classification, wrapped with the residual variance estimation framework.

Random Forest with ResidualDouble (Gressmann & Kiraly, 2018) was tuned over tree depth ($\text{max_depth} \in [3, 50]$), minimum samples to split ($\text{min_samples_split} \in [2, 150]$), minimum samples at leaves ($\text{min_samples_leaf} \in [1, 100]$), minimum impurity decrease ($\text{min_impurity_decrease} \in [0.0, 0.1]$), and maximum features ($\text{max_features} \in [0.5, 1.0]$).

Decision Tree with ResidualDouble was tuned over depth, split constraints, leaf size, and impurity decrease, using the same ranges as Random Forest.

NGBoost for regression used a decision tree regressor as its base learner with the same hyperparameter space as in classification.

CADET was tuned over tree depth ($\text{max_depth} \in [3, 50]$), minimum samples to split ($\text{min_samples_split} \in [2, 150]$), and minimum samples at leaves ($\text{min_samples_leaf} \in [1, 100]$).

CDTree was used with their default configurations without hyperparameter tuning, as suggested by the original implementation.

For Random Forest, Decision Tree, NGBoost, and CADET in both settings, categorical features were one-hot encoded via a preprocessing pipeline, while XGBoost, Partition Tree, and Partition Forest handles categorical features natively.

D.3. Extended classification and regression results

Table 5 reports the classification accuracy of the evaluated methods. Tables 6 and 7 summarize the regression performance in terms of log-loss and RMSE, respectively, reporting mean and standard deviation across five-fold cross-validation.

Across both classification and regression, the results follow a consistent trend. Partition Trees outperform CART for both probabilistic and point-estimation tasks. Among ensemble methods, however, performance depends on the metric: Partition Forests achieve lower log-loss, whereas Random Forests obtain higher classification accuracy and lower RMSE in regression.

Table 5. Accuracy results over 5-fold cross-validation for ensemble and non-ensemble tree methods on classification tasks (mean \pm std). Higher is better. Best for ensemble and non-ensemble in bold. The last row represents the average ranking of each method in its group. Underline indicates statistical ties according to a paired t-test at the 5% significance level (run separately within ensemble and non-ensemble groups).

	Non-ensemble models			Ensemble models			
	CART	Partition Tree	Partition Forest	Random Forest	NGBoost	XGBoost	
iris	0.8067 \pm 0.1921	<u>0.7800 \pm 0.2694</u>	<u>0.8267 \pm 0.2966</u>	0.9600 \pm 0.0279	<u>0.9400 \pm 0.0279</u>	<u>0.9467 \pm 0.0298</u>	
breast	0.7134 \pm 0.0630	<u>0.6924 \pm 0.0389</u>	<u>0.7273 \pm 0.0362</u>	0.7552 \pm 0.0633	<u>0.7097 \pm 0.0216</u>	<u>0.7307 \pm 0.0322</u>	
wine	<u>0.5566 \pm 0.0369</u>	0.5929 \pm 0.0336	<u>0.6717 \pm 0.0375</u>	0.6754 \pm 0.0319	<u>0.5835 \pm 0.0327</u>	<u>0.6391 \pm 0.0481</u>	
digits	<u>0.7217 \pm 0.0821</u>	0.8692 \pm 0.0184	<u>0.9499 \pm 0.0099</u>	0.9750 \pm 0.0034	<u>0.8809 \pm 0.0208</u>	<u>0.9666 \pm 0.0052</u>	
spam	<u>0.8946 \pm 0.0245</u>	0.9287 \pm 0.0113	<u>0.9452 \pm 0.0126</u>	<u>0.9502 \pm 0.0132</u>	<u>0.9300 \pm 0.0121</u>	0.9515 \pm 0.0094	
support2	<u>0.8949 \pm 0.0040</u>	0.8975 \pm 0.0066	<u>0.9058 \pm 0.0046</u>	<u>0.9040 \pm 0.0058</u>	<u>0.9046 \pm 0.0067</u>	0.9088 \pm 0.0068	
letter	<u>0.6627 \pm 0.0112</u>	0.8310 \pm 0.0589	<u>0.8854 \pm 0.0043</u>	0.9629 \pm 0.0039	<u>0.7178 \pm 0.0534</u>	<u>0.9521 \pm 0.0051</u>	
bank	<u>0.9020 \pm 0.0050</u>	0.9029 \pm 0.0036	<u>0.9064 \pm 0.0029</u>	<u>0.9049 \pm 0.0046</u>	<u>0.8996 \pm 0.0045</u>	0.9092 \pm 0.0042	
adult	0.5921 \pm 0.0056	<u>0.5890 \pm 0.0066</u>	<u>0.5959 \pm 0.0054</u>	<u>0.5985 \pm 0.0053</u>	<u>0.5910 \pm 0.0050</u>	0.6012 \pm 0.0046	
Avg. rank	1.67	1.33	2.78	1.78	3.78	1.67	

Table 6. Log-loss results over 5-fold cross-validation for ensemble and non-ensemble tree methods on regression task. Best for each group in bold (lower is better). The last row represents the average ranking of each method on its group. Underline indicates statistical ties according to a paired t-test at the 5% significance level (run separately within ensemble and non-ensemble groups)

	Non-ensemble models				Ensemble models			
	Partition Tree	CART	CADET	CDTree	Partition Forest	Random Forest	NGBoost	XGBoost
diabetes	<u>5.6508 \pm 0.1087</u>	17.9335 \pm 2.4880	<u>5.5928 \pm 0.1432</u>	5.5782 \pm 0.0589	5.4860 \pm 0.1023	14.2150 \pm 2.4289	<u>5.5002 \pm 0.1079</u>	16.8124 \pm 3.1159
boston	<u>2.9033 \pm 0.1741</u>	8.3920 \pm 3.3271	<u>2.8919 \pm 0.1841</u>	2.8778 \pm 0.1419	2.5250 \pm 0.1345	4.6011 \pm 1.0842	<u>2.5861 \pm 0.1407</u>	4.5953 \pm 1.3377
energy	2.3589 \pm 0.1813	<u>1.6711 \pm 0.0383</u>	<u>10.8069 \pm 18.6170</u>	1.5485 \pm 0.1586	2.0618 \pm 0.0746	1.5516 \pm 0.0256	0.5957 \pm 0.3404	1.5341 \pm 0.0256
concrete	<u>3.7016 \pm 0.0552</u>	7.4455 \pm 0.9024	3.5214 \pm 0.1712	<u>3.6594 \pm 0.0565</u>	3.3640 \pm 0.0350	3.8643 \pm 0.3960	3.1138 \pm 0.1402	<u>3.4367 \pm 0.3310</u>
kin8nm	<u>-0.1780 \pm 0.0223</u>	9.4188 \pm 0.1536	<u>-0.2193 \pm 0.0370</u>	<u>-0.1818 \pm 0.0121</u>	<u>-0.4511 \pm 0.0168</u>	3.2966 \pm 0.1232	-0.4912 \pm 0.0338	2.0540 \pm 0.2646
air	2.1247 \pm 0.1141	13.4880 \pm 1.0048	<u>13.7818 \pm 17.5444</u>	6.4168 \pm 0.0003	2.0172 \pm 0.0958	11.3537 \pm 0.8769	5.6210 \pm 1.5702	12.2496 \pm 1.0273
power	2.8695 \pm 0.0158	3.1347 \pm 0.1002	<u>2.9034 \pm 0.1002</u>	2.9259 \pm 0.0252	<u>2.5951 \pm 0.0163</u>	2.6344 \pm 0.0577	2.7688 \pm 0.1316	2.5905 \pm 0.0579
naval	-4.3766 \pm 0.1484	4.6865 \pm 0.2227	-4.7819 \pm 0.0813	-4.2938 \pm 0.0344	-4.7186 \pm 0.0105	-4.9824 \pm 0.0126	-5.0528 \pm 0.0429	-4.9348 \pm 0.0105
california	0.6853 \pm 0.0210	7.0717 \pm 0.3637	0.8837 \pm 0.1582	0.5829 \pm 0.0213	0.4176 \pm 0.0192	3.1070 \pm 0.1352	0.5225 \pm 0.0318	2.5088 \pm 0.1484
protein	2.2210 \pm 0.0176	12.3085 \pm 0.1981	3.1323 \pm 0.2200	2.1841 \pm 0.0204	<u>2.1011 \pm 0.0171</u>	6.1910 \pm 0.0415	2.7906 \pm 0.0261	7.2314 \pm 0.1174
Avg. rank	2.30	3.70	2.30	1.70	1.90	3.30	1.80	3.00

Table 7. RMSE results over 5-fold cross-validation for ensemble and non-ensemble tree methods on regression task (mean \pm std). Best for each group in bold (lower is better). The last row represents the average ranking of each method on its group. Underline indicates statistical ties according to a paired t-test at the 5% significance level (run separately within ensemble and non-ensemble groups)

	Non-ensemble models				Ensemble models			
	Partition Tree	CART	CADET	CDTree	Partition Forest	Random Forest	NGBoost	XGBoost
diabetes	60.8469 \pm 3.7035	66.0686 \pm 4.3637	<u>63.3747 \pm 2.7527</u>	<u>63.8697 \pm 4.3191</u>	56.1571 \pm 2.0060	<u>56.6220 \pm 2.5885</u>	<u>57.3078 \pm 2.2566</u>	63.0091 \pm 2.1380
boston	<u>4.9451 \pm 0.4267</u>	4.5558 \pm 1.3400	<u>4.5706 \pm 0.8286</u>	<u>4.8580 \pm 0.8571</u>	4.1597 \pm 0.6955	<u>3.1755 \pm 0.6638</u>	<u>3.5388 \pm 0.7070</u>	3.1280 \pm 0.6539
energy	4.4647 \pm 0.3512	1.0085 \pm 0.0861	0.6813 \pm 0.0436	4.8769 \pm 0.1724	4.5773 \pm 0.4197	0.4788 \pm 0.0322	0.4597 \pm 0.0491	0.3367 \pm 0.0332
concrete	<u>8.1692 \pm 0.4043</u>	<u>8.3429 \pm 0.4559</u>	7.5666 \pm 0.5510	9.0076 \pm 0.8059	7.4584 \pm 0.5900	5.0355 \pm 0.6595	<u>5.3934 \pm 0.5112</u>	4.4791 \pm 0.6402
kin8nm	0.1859 \pm 0.0045	0.2046 \pm 0.0033	0.1949 \pm 0.0024	0.2121 \pm 0.0033	0.1575 \pm 0.0020	0.1410 \pm 0.0013	0.1594 \pm 0.0021	0.1241 \pm 0.0028
air	60.3952 \pm 4.3365	53.8907 \pm 2.3661	56.1893 \pm 1.6509	98.0611 \pm 0.0901	54.6616 \pm 5.2004	47.8334 \pm 2.2149	53.2590 \pm 2.3771	50.4488 \pm 2.4324
power	4.0051 \pm 0.1611	4.4409 \pm 0.1662	4.1441 \pm 0.1351	4.5171 \pm 0.1261	3.6756 \pm 0.1969	3.3166 \pm 0.1501	3.6042 \pm 0.1185	3.1985 \pm 0.1590
naval	0.0029 \pm 0.0002	0.0113 \pm 0.0001	0.0023 \pm 0.0002	0.0039 \pm 0.0001	0.0026 \pm 0.0002	0.0009 \pm 0.0001	0.0017 \pm 0.0001	0.0012 \pm 0.0000
california	0.5691 \pm 0.0116	0.7166 \pm 0.0100	0.6109 \pm 0.0244	0.6383 \pm 0.0096	0.5574 \pm 0.0146	0.5048 \pm 0.0104	0.4881 \pm 0.0123	0.4645 \pm 0.0157
protein	4.3938 \pm 0.0385	5.1811 \pm 0.0364	4.7821 \pm 0.1181	4.6290 \pm 0.0430	4.7202 \pm 0.0249	3.5096 \pm 0.0176	4.2972 \pm 0.0343	3.8454 \pm 0.0387
Avg. rank	1.90	2.90	1.80	3.40	3.60	1.90	2.90	1.60

E. Runtime comparison

To evaluate the computational efficiency of the proposed Partition Tree method, we compared its runtime with CADET and CDTree on the Physicochemical Protein dataset. We measured training time across three random sample sizes ($n \in \{100, 1000, 10000\}$), repeating each configuration five times with different random seeds to account for variability.

All models were configured without hyperparameter tuning, using permissive settings (a large maximum depth/iterations and a minimum samples per leaf of 1) to ensure the runtime reflects the inherent algorithmic complexity rather than early stopping behavior.

Figure 4 presents the training time as a function of sample size on a log-log scale. Partition Tree consistently achieves the fastest training times across all sample sizes, being approximately 5× faster than CADET and 25× faster than CDTree at $n = 10000$. The shaded regions indicate the range between the minimum and maximum observed runtimes across runs.

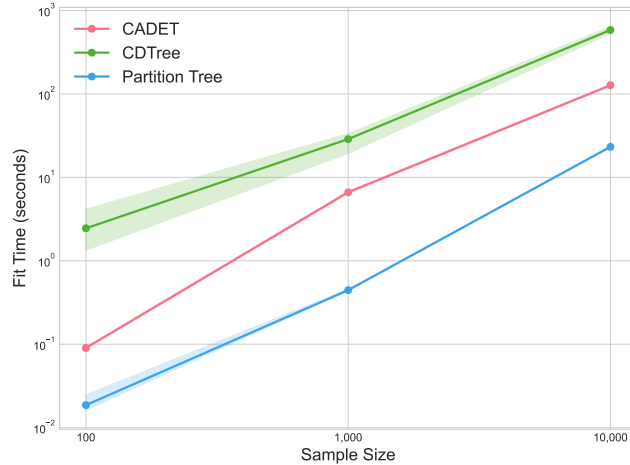


Figure 4. Training time comparison on the Physicochemical Protein dataset across different sample sizes. Solid lines indicate mean runtime; shaded regions show the range across five runs. Partition Tree demonstrates consistent computational efficiency and scales favorably compared to both CADET and CDTree.

F. Gain-based Feature Importance

Partition Trees retain the interpretability advantages of classical decision trees: each internal node applies a single-coordinate test, and the learned model is a piecewise-constant conditional density on the induced leaves.

To summarize which *covariates* drive the conditional density estimate, we use a gain-based feature importance that is aligned with the training objective. Recall that every accepted split is chosen to maximize the empirical log-loss gain \widehat{G} (Equation (10)). For a fitted tree T and a covariate coordinate $j \in \{1, \dots, d_x\}$, define the unnormalized importance

$$\tilde{I}_j(T) := \sum_{s \in \text{Int}(T)} \widehat{G}_s \mathbf{1}\{\text{split } s \text{ uses } X_j\},$$

where $\text{Int}(T)$ is the set of internal nodes and \widehat{G}_s is the gain realized at node s . We then report the normalized importance

$$I_j(T) := \frac{\tilde{I}_j(T)}{\sum_{s \in \text{Int}(T)} \widehat{G}_s}, \quad \sum_{j=1}^{d_x} I_j(T) = 1.$$

This definition matches the standard ‘‘impurity decrease’’ importances used for CART, with \widehat{G} replacing the classification or regression impurity. Because Partition Trees also allow Y -splits to refine the outcome partition, we restrict I_j to *X-splits only* so that importances reflect how the model adapts to the covariates (rather than how it discretizes the outcome).

F.1. Comparison with CADET importances

CADET selects splits using a cross-entropy criterion, so its gain has the same log-loss structure as ours. Empirically, the resulting importances are closely aligned across regression benchmarks: Figure 5 plots CADET importances against Partition Tree importances (each point is one feature in one dataset), and most points concentrate near the equality line, indicating broad agreement in which covariates matter and at what scale.

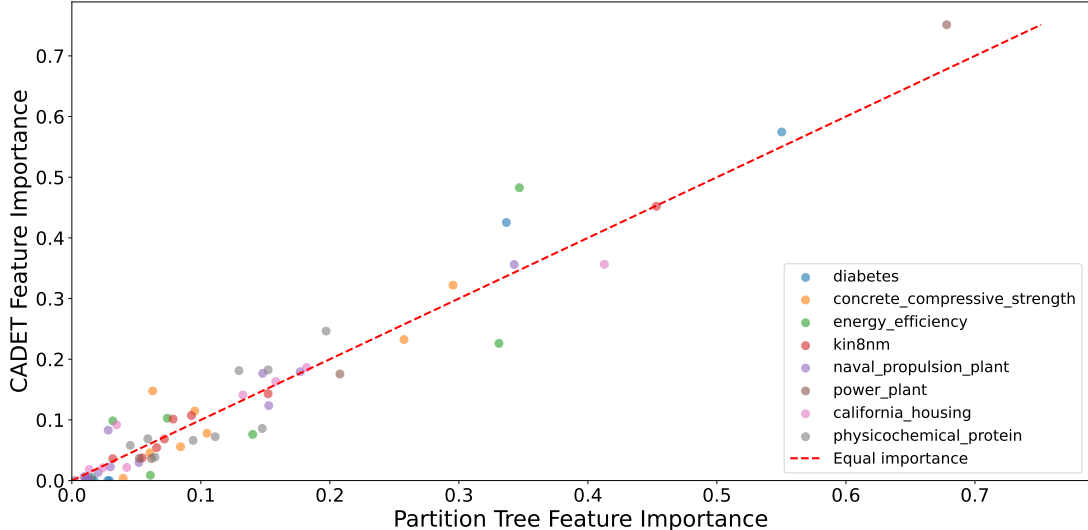


Figure 5. Normalized gain-based feature importances for Partition Tree vs. CADET across regression datasets for the first fold of the cross-validation. Each marker corresponds to a single feature on a given dataset; the dashed line indicates equal importance. The Air Quality dataset is omitted because CADET returned NaN feature importances.

F.2. Example: California Housing

As a concrete illustration, Figure 6 shows the normalized features importance on California Housing for the Partition Tree and CADET. Both methods identify `MedInc` as the dominant predictor, followed by geographic covariates (`Longitude`, `Latitude`) and occupancy statistics, with the remaining variables contributing less. This qualitative agreement is representative of the trends observed across datasets.

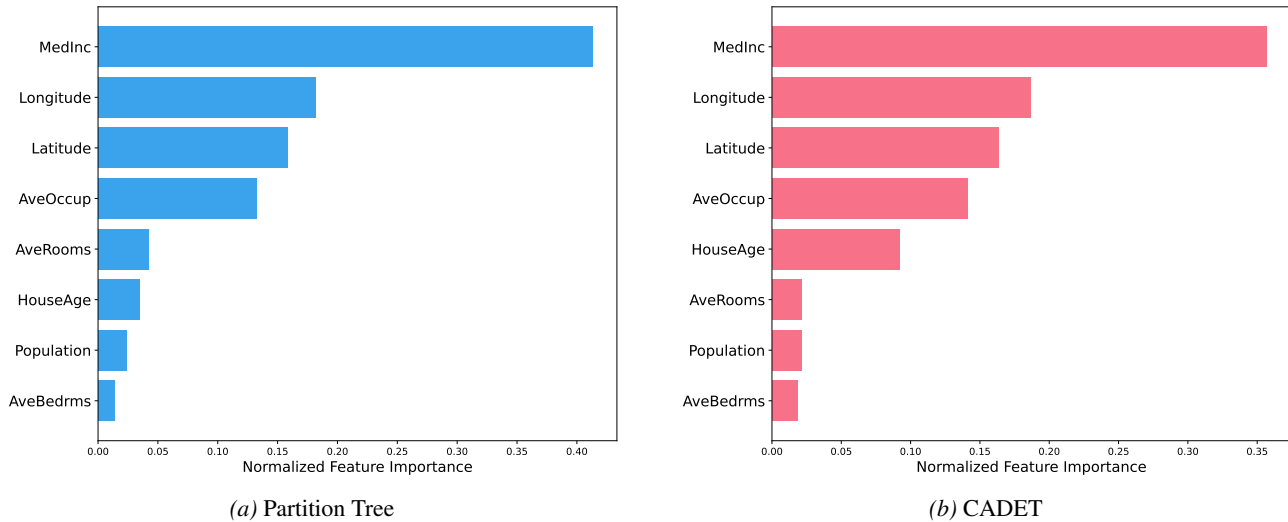


Figure 6. Normalized gain-based feature importance for the California Housing dataset. Both Partition Tree and CADET place MedInc as most important, followed by geographic covariates and occupancy-related features.

Caveat. As with standard impurity-based importance, gain-based scores can be affected by correlated predictors and by the set of admissible split tests. We therefore use them as a descriptive diagnostic of how the learned partition adapts to X , rather than as a causal attribution.

G. Effect of Exploration Splits on Probabilistic Regression

We report an ablation comparing the default gain-based Partition Tree (no exploration splits) against a variant that allocates a nonzero exploration budget. For the exploration variant, we introduce a hyperparameter $\alpha \in [0.1, 0.9]$ and set the exploration budget to $k_{N,e} = \lfloor \alpha k_N \rfloor$. Thus, the total split budget is $k_N + k_{N,e}$, where k_N splits are selected by empirical gain maximization and $k_{N,e}$ splits are diameter-reducing exploration splits. Results are reported as mean \pm standard deviation of the negative log-likelihood over 5-fold cross-validation (lower is better).

Table 8. Regression log-loss (mean \pm std) for Partition Tree with and without exploration splits. Lower is better. Best is in bold. Underline indicates statistical ties according to a paired t-test at the 5% significance level.

Dataset	Partition Tree	Partition Tree (+Exploration)
Diabetes	5.6508 \pm 0.1087	5.8352 \pm 0.0739
Boston	2.9033 \pm 0.1741	3.2099 \pm 0.1676
Energy	2.3589 \pm 0.1813	2.9605 \pm 0.2133
Concrete	3.7016 \pm 0.0552	4.0207 \pm 0.0641
kin8nm	-0.1780 \pm 0.0223	-0.0710 \pm 0.0219
Air	2.1247 \pm 0.1141	2.7802 \pm 0.1282
Power	2.8695 \pm 0.0158	3.0404 \pm 0.0215
Naval	-4.3766 \pm 0.1484	<u>-4.3714 \pm 0.0455</u>
California	0.6853 \pm 0.0210	0.8973 \pm 0.0302
Protein	2.2210 \pm 0.0176	2.3072 \pm 0.0175